Targeted therapy impairing oncogenic KRAS signalling by inhibition of KRAS–PDEδ interaction

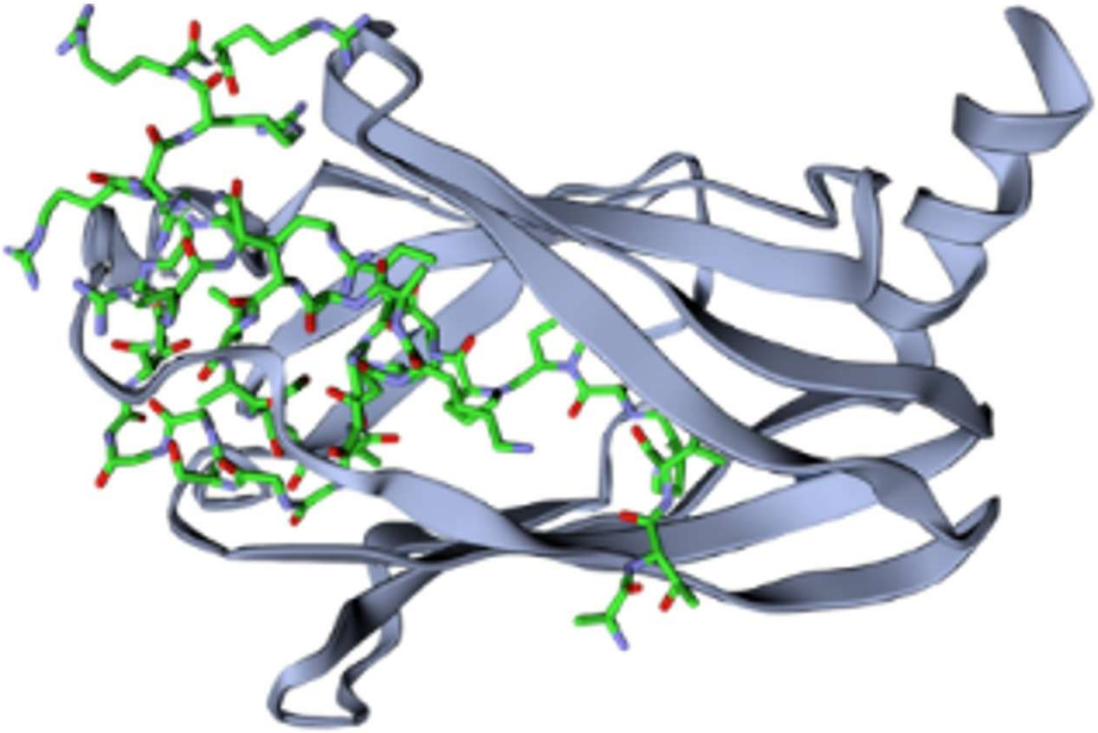

Li Tsz Yee, Kwan Ho Chit, Wong Sum Yee

Content

Abstract

This project aims to develop anti-cancer drugs by targeting PDEδ, which regulates KRAS signaling pathway in cancer cell. RFdiffusion, ProteinMPNN and Alphafold2 are used to generate peptide sequences. Next, DynamicBind is used to compare the binding affinity of potential peptides. Then, five peptide drugs were chosen and expressed by BL21. Finally, A549, a lung cancer cell line, was used to test the effectiveness of the AI-generated peptides.

In a two days treatment, ACP5, which is found to be the most promising peptide drug in our study, induced an 80% inhibition in viability of 2D cancer cells and 20% inhibition in viability of 3D Multi-Cellular Tumor Spheroid (MCTS). Hence, ACP5 is named KAPI (KRAS and PDEδ Inhibitor). With the supplement of KAPI, a reduced concentration of Cisplatin is shown to achieve the same percentage of inhibition on cancer cell viability as that at its IC50. As a lower concentration of Cisplatin can be used, KAPI can reduce Cisplatin's side effects in combination therapy.

1. Introduction

1.1 A new era of sophisticated ML algorithms in biomedicine

Cancer is one of the top killers in the world. According to the World Health Organisation, approximately 10 million deaths in the year 2020 are caused by cancer, representing one sixth of the total number of deaths recorded in the same year worldwide.[1] The research in cancer drug has utmost importance in saving life for decades. With the rapid evolution of AI, ML algorithms in biomedicine significantly impact drug discovery.[2] The rise of bioinformatics and AI tools in peptide research has spurred the development of advanced methodologies in the exploration of novel therapeutics.

1.2 Background of PDEδ as molecular target for cancer drug development

KRAS mutation is the most frequent oncogenic alteration in human cancers including pancreatic, colorectal, lung adenocarcinomas and urogenital cancers. [3] It alternates between "on" and "off" conformations, differing by the binding with GTP and GDP respectively, under normal conditions. The oncogenic form of KRAS partially inhibits the activity of GTPase, a protein responsible for converting GTP to GDP. This results in a constant active state of KRAS, which tends to prefer binding with GTP over GDP. As a result, GTP-bounded KRAS can engage in cytoplasmic signal transduction constantly, most commonly through downstream pathways RAL, RAF-MEK-ERK, and Pl3K [4], directly resulting in abnormal proliferation, and this can be done without a growth factor. [5]

Therefore, KRAS presents a promising molecular target for the development of cancer therapeutics. However, KRAS has been deemed a challenging therapeutic target, even "undruggable", after drug-

targeting efforts over the past decades. [6] Various studies have previously deemed KRAS an unideal candidate for cancer treatment. This is due to its unusually smooth structure and lack of significant, otherwise shallow drug-binding sites.

Hence, the hope of inhibiting KRAS activity is shifted to another contributor to KRAS signaling: the phosphodiesterase-delta (PDEδ). Signal transduction of KRAS in its active form is highly dependent on its localisation to the cell membrane. PDEδ sustains the spatial organization of KRAS by facilitating its diffusion in the cytoplasm and regulating its localization to endomembrane. PDEδ acts as a solubilisation factor which binds to the farnesyl-tail of KRAS. Its hydrophobic pocket can interact with a farnesylated hydrophobic cysteine residue at the C terminus of KRAS, hence enabling its movement and diffusion in the cytoplasm, and sustaining its spatial distribution on the cell membrane. This allows KRAS signaling to take place. [7] So, PDEδ can be a potential target for inhibiting KRAS activity. [8]

1.3 Choice of lung cancer as the research focus

In Non-Small Cell Lung Cancer (NSCLC) specifically, KRAS mutation has a frequency of around 30%, and the most common KRAS mutations in NSCLC are G12C (13.43%), which is of common occurrence in current and former smokers. and G12D (29.19%, 13.03% in NSCLC) [9], these oncogenic KRAS mutations develop unique metabolic dependencies on nutrients to support tumor metabolism and cell proliferation.

1.4 The objective

In this study, a potentially potent peptide drug against PDEδ is developed to inhibit cancer cell viability, with the assistance of bioinformatics tools. All peptide drug inserts have been incorporated into our pET plasmid and then transformed into BL21 for protein expression. Those peptides would be purified and collected for cytotoxicity test. The most promising ACP found is named KAPI, the KRAS and PDEδ Inhibitor.

1.5 Drug screening using Multi-Cellular Tumor Spheroid (MCTS)

The tumor microenvironment (TME) is a key factor of tumor aggressiveness and resistance. However, traditional 2D cell culture cannot fully simulate the condition of lung cancer tumor in humans. The cell-cell interactions, which are crucial for maintaining normal cellular functions and gene expression, are absent in 2D culture. [10] Generally, 2D cell culture will also have a higher drug sensitivity than a tumor due to a higher surface area to volume ratio which causes more cells to be exposed to drug containing medium. Hence, 3D culture is much more representative of in vivo tumors in which inner cells have less access to nutrients and oxygen compared to the outer layer, forming a natural gradient. [11] Hence, KAPI's effectiveness is studied with cancer cell line A549 in both 2D and 3D cell culture.

1.6 More about our project ideas and development

In this research, to model the impact of anticancer peptides KAPI on the in-vitro growth of cancer cell A549, an Ordinary Differential Equation (ODE) model is developed. The content is discussed in Appendix I - ODE Model.

To promote our findings and engage with the community, the team has developed two sets of promotion materials, which were used in educational activities organized in schools. The content is discussed in Appendix II - Education Promotion.

May the team express sincere gratitude to local Scientists for their invaluable support and guidance throughout this research. The process is recorded in our learning journey and they are discussed in Appendix III – Attribution.

2. Materials and Methods

2.1 Structure of Phosphodiesterase-delta (PDEδ)

Experimentally solved structure of PDEδ (PDB ID: 4JV6) was the starting point of the structure-based design. PDEδ is comprised of 150 amino acids and it has a beta-sandwich immunoglobulin fold, which contains a hydrophobic pocket capable of binding to the farnesyl group. [12], [13]

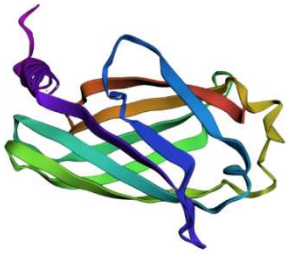

Figure 2.1 - Structure of PDEδ (Predicted by AlphaFold2)

2.1.1 RFdiffusion

RFdiffusion is used to generate peptide backbones that could potentially bind to the target residues in its binder design mode. By entering the length of binder as 20 amino acids and the amino acid sequence of PDEδ, RFdiffusion generated a protein backbone that may bind to it for further investigation. [14]

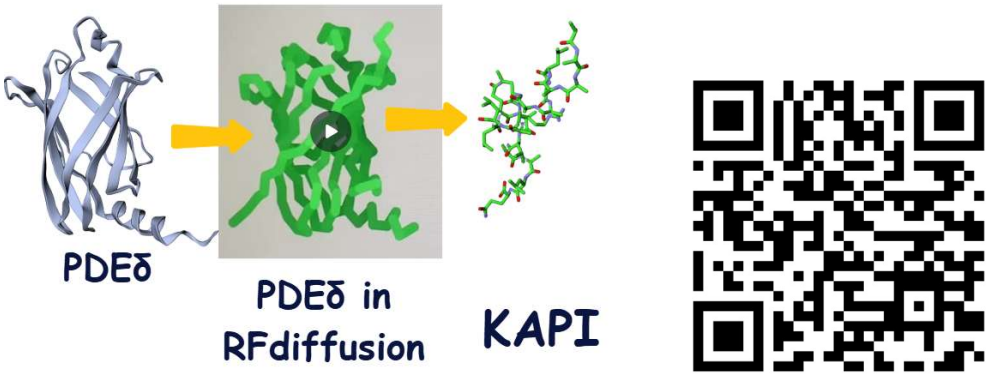

Figure 2.2 - 2D animation of the protein diffusion process over each timestep.

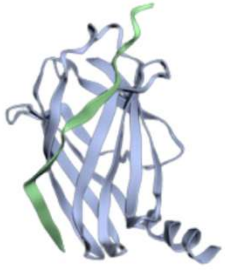

Figure 2.3 - Protein backbone generated from RFdiffusion. (Green: PDEδ, Grey: Protein backbone)

2.1.2 ProteinMPNN

After the peptide backbones are generated in RFdiffusion, ProteinMPNN is used to predict sequences of the 16 peptides backbone. [15] 64 sequences are generated for each backbone, and 1024 (64*16) sequences are subsequently passed to AlphaFold2-multimer for further screening.

2.1.3 AlphaFold2

Using the multimer mode, AlphaFold2 has been utilized to predict the most probable sequences bound to PDEδ [16]; for each predicted PDEδ-peptide complex, a Predict Aligned Error (PAE) is given. It represents the overall distance error of each predicted coordinate, i.e. the distance between the predicted coordinate and the actual coordinate. 16 peptides with the lowest PAE score are selected to narrow down the number of possible working peptides. The 16 potential candidates, as shown in Table 2.1 are selected for further screening.

Table 2.1 - 16 potential candidates from AlphaFold2

>1 SHISAVGPAAFTAEEIAESL >2 PVLVLPQAVLVAAPGELEEF >3 MTTLPPPPRFVGEDRSEELE >4 GSEIAAARLAAELARLAELE >5 AAAALAAALRALLQALAALQ >6 SPEELERALRRISVAPDQSG >7 MPKVTVNSALAAAGAGHFGK >8 MTEEQKKLAESVAKMRIVAP	>9 TIIKLVPGPDAAALAAETPR >10 SIRLTLIGDEELAKKVAEEE >11 MELKISGSEKSELMEELEKE >12 ATVPAPPKIDKAAQLASAAK >13 GLSFSFDFAAARAAREAELA >14 MIDLKITGGGGPGMAVSAGV >15 AEAAAAATEALRAAQAAAAE >16 SLVLPPVLLKRSSGGAGPAP

2.2 Screening of cell-penetrating activity

Owing to the fact that our drug target PDEδ, which is intracellular, the peptide drug should show good cell-penetrating activity. Then, AI database CellPPD can be used to evaluate peptide's cell-penetrating activity. [17] The Support Vector Machine (SVM) score is used to predict the likelihood that a peptide is a cell-penetrating peptide (CPP). The SVM score typically ranges from -1 to +1. A higher positive score indicates a higher likelihood that the peptide is a CPP. A lower or negative score suggests a lower likelihood of being a CPP:

High SVM Score (e.g., +0.8): This peptide is very likely to be a CPP.
Moderate SVM Score (e.g., +0.3): This peptide has a moderate likelihood of being a CPP.
Low SVM Score (e.g., -0.2): This peptide is unlikely to be a CPP.

The 16 peptides and four peptides (DPV6, R8, pVEC, and MAP) [18] known for its cell-penetrating capability are analyzed. The results are shown in Table 2.2.

Table 2.2 - SVM score of the 16 peptides and four peptides (DPV6, R8, pVEC, and MAP) known for its cell-penetrating capability

Identity	Amino acid sequence	SVM score
Sequence 1	SHISAVGPAAFTAEEIAESL	-0.71
Sequence 2	PVLVLPQAVLVAAPGELEEF	-0.75
Sequence 3	MTTLPPPPRFVGEDRSEELE	-0.61
Sequence 4	GSEIAAARLAAELARLAELE	-0.44
Sequence 5	AAAALAAALRALLQALAALQ	-0.22
Sequence 6	SPEELERALRRISVAPDQSG	-0.34
Sequence 7	MPKVTVNSALAAAGAGHFGK	-0.61
Sequence 8	MTEEQKKLAESVAKMRIVAP	-0.51
Sequence 9	TIIKLVPGPDAAALAAETPR	-0.2
Sequence 10	SIRLTLIGDEELAKKVAEEE	-0.6
Sequence 11	MELKISGSEKSELMEELEKE	-0.62
Sequence 12	ATVPAPPKIDKAAQLASAAK	-0.16
Sequence 13	GLSFSFDFAAARAAREAELA	-0.33
Sequence 14	MIDLKITGGGGPGMAVSAGV	-0.82
Sequence 15	AEAAAAATEALRAAQAAAAE	-0.57
Sequence 16	SLVLPPVLLKRSSGGAGPAP	0.04
DPV6	GRPRESGKKRKRKRLKP	1
R8	RRRRRRRR	1.23
pVEC	LLIILRRRIRKQAHAHSK	1.27
MAP	KLALKLALKALKAALKLA	1.47

The amino acid sequences of the 16 AI-generated peptides exhibit negative SVM scores, suggesting a low probability of their classification as cell-penetrating peptides (CPPs). In contrast, the four peptides known for their cell-penetrating capabilities demonstrate high SVM scores, with each scoring 1 or higher, indicating a strong likelihood of being classified as CPPs

Given the proposed intracellular mechanism of the de novo design peptide, the situation needs attention. Further optimization may be needed to enhance the cell-penetrating capabilities of these peptides.

2.3 Design of the fusion peptide

Fusion peptides are increasingly being explored in cancer peptide drug research. A fusion peptide might include a Cell-Penetrating Peptide (CPP), which facilitates the entry of the therapeutic agent into cancer cells, along with a therapeutic domain that induces cell death. [19] By fusing these targeting sequences with therapeutic peptides, researchers can improve the specificity and penetration of the drug into the Tumour Micro-Environment (TME).

To improve the cell penetrating activity of our ACPs, a Cell-Penetrating Peptide is added. The schematic diagram is as follows:

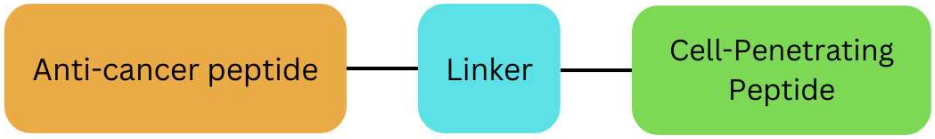

Figure 2.4 - Schematic diagram of our fusion peptide

Linker: The flexible linker 'GGSGGGSG' in between the AI-generated peptide and the Cell-Penetrating Peptide is used with reference to iGem Registry of Standard Biological Parts (Part:BBa_K243005). The linker is designed by Freiburg Bioware from iGEM09_Freiburg_bioware in the year 2009. [20]

Polyarginine Cell-Penetrating Peptide: Peptides, especially intracellular functional peptides that can play a particular role inside a cell, have attracted attention as promising materials to control cell fate. However, hydrophilic materials like peptides are difficult for cells to internalize. [21] Octaarginine (R8) as a Polyarginine Cell-Penetrating Peptide (CPP) is reported to enhance peptide's ability to cross the cell membrane and deliver cargo. [22] Hence, 'RRRRRRRR' is used as our Cell-Penetrating Peptide sequence for penetrating cell membrane and entering the cell. The backbone of the fusion peptides is designed to have both promising ability to target intra-cellular PDEδ and enter cancer cells effectively.

In conclusion, by incorporating cell-penetrating peptides into the AI-generated peptide, the resulting fusion peptide (Table 2.3) should demonstrates an enhanced ability to infiltrate cancer cells. As a result, the overall efficacy in anticancer activity should be significantly increased.

Table 2.3 - Sequence of ACPs after modification (Linker, Cell-Penetrating Peptides)

Identity	**Amino acid sequence**
ACP1	SHISAVGPAAFTAEEIAESLGGSGGGSGRRRRRRRR
ACP2	PVLVLPQAVLVAAPGELEEFGGSGGGSGRRRRRRRR
ACP3	MTTLPPPPRFVGEDRSEELEGGSGGGSGRRRRRRRR
ACP4	GSEIAAARLAAELARLAELEGGSGGGSGRRRRRRRR
ACP5	AAAALAAALRALLQALAALQGGSGGGSGRRRRRRRR
ACP6	SPEELERALRRISVAPDQSGGGSGGGSGRRRRRRRR
ACP7	MPKVTVNSALAAAGAGHFGKGGSGGGSGRRRRRRRR
ACP8	MTEEQKKLAESVAKMRIVAPGGSGGGSGRRRRRRRR
ACP9	TIIKLVPGPDAAALAAETPRGGSGGGSGRRRRRRRR
ACP10	SIRLTLIGDEELAKKVAEEEGGSGGGSGRRRRRRRR
ACP11	MELKISGSEKSELMEELEKEGGSGGGSGRRRRRRRR
ACP12	ATVPAPPKIDKAAQLASAAKGGSGGGSGRRRRRRRR
ACP13	GLSFSFDFAAARAAREAELAGGSGGGSGRRRRRRRR
ACP14	MIDLKITGGGGPGMAVSAGVGGSGGGSGRRRRRRRR
ACP15	AEAAAAATEALRAAQAAAAEGGSGGGSGRRRRRRRR
ACP16	SLVLPPVLLKRSSGGAGPAPGGSGGGSGRRRRRRRR

2.4 Screening of binding affinity towards PDEδ

While significant advances have been made in predicting static protein structures, the inherent dynamics of proteins, modulated by ligands, are crucial for understanding protein function and facilitating drug discovery. [23] Hence, the amino acid sequence of the 16 fusion peptides are screened by DynamicBind to study their affinity for the protein-ligand interactions with PDE δ . In DynamicBind, cLDDT and binding affinity are provided for analysis:

Contact Local Distance Difference Test (cLDDT): This score assesses the accuracy of the predicted binding complex by measuring how well the predicted protein-ligand contacts match the native structure. Higher cLDDT values indicate a closer match to the true binding pose.

Binding Affinity: This metric estimates the strength of the interaction between the protein and ligand, using a predicted affinity value derived from training on experimental binding data. Higher values indicate a stronger predicted affinity, suggesting a more favorable binding interaction in potential drug candidates:

High Binding Affinity: Higher values (e.g., above 8.0) suggest strong interactions.
Low Binding Affinity: Lower values (e.g., below 7.0) indicate weaker interactions.

5 fusion peptides for chosen for their relatively high cLDDT and binding affinity. The data are shown in Table 2.4.

Table 2.4 - cLDDT and binding affinity of ACPs

Identity	Sequence	cLDDT	Binding Affinity
ACP1	SHISAVGPAAFTAEEIAESLGGSGGGSGRRRRRRRR	0.383	7.99
ACP5	AAAALAAALRALLQALAALQGGSGGGSGRRRRRRRR	0.371	8.195
ACP7	MPKVTVNSALAAAGAGHFGKGGSGGGSGRRRRRRRR	0.353	9.205
ACP11	MELKISGSEKSELMEELEKEGGSGGGSGRRRRRRRR	0.324	8.399
ACP12	ATVPAPPKIDKAAQLASAAKGGSGGGSGRRRRRRRR	0.330	8.623

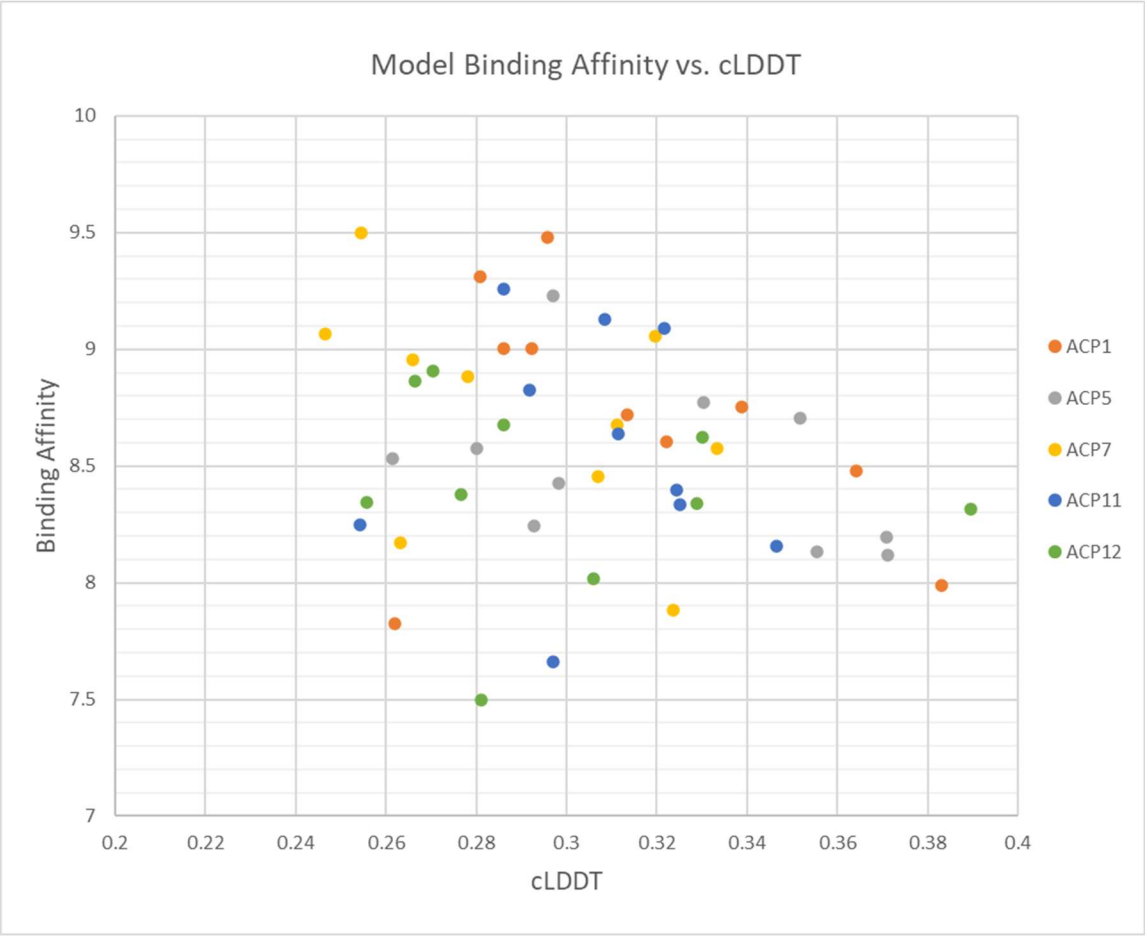

Figure 2.5 - cLDDT and binding affinity of ACPs

The binding affinity is crucial for anti-cancer peptide to exert its effect. Strong binding affinity leads to more efficient receptor activation, enabling the ligand to induce conformational changes and initiate signaling pathways. [24] Besides, high-affinity ligands are generally more potent, achieving desired effects at lower concentrations and resulting in a longer duration of action, which reduces dosage and side effects in drug development.

ACP1 has the highest cLDDT score, signifying a closer alignment with the binding pose. Following this, ACP5 ranks second in cLDDT score and demonstrates a binding affinity value of 8.195, indicating a robust interaction with PDEδ. ACP11 similarly has a relatively high cLDDT and binding affinity. Additionally, both ACP7 and ACP12 possess cLDDT scores exceeding 0.3 and binding affinity scores surpassing 8.5 concurrently, reflecting a significant capacity for binding with PDEδ. Finally, ACP1, ACP5, ACP7, ACP11, ACP12 are chosen for expression and cytotoxicity test.

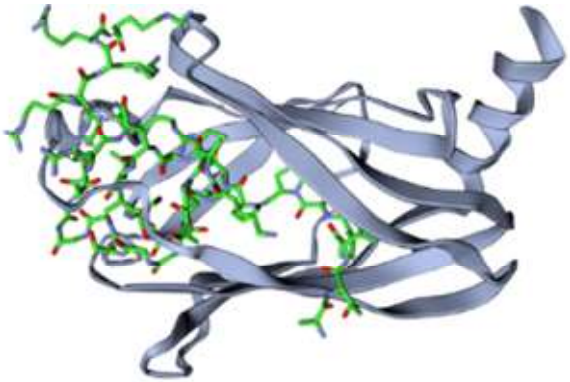

Figure 2.6 - The ligand (ACP5) binding with PDEδ with high cLDDT and binding affinity

2.5 Plasmid Design

The plasmid used contains an insert of five fusion peptides respectively, which were ligated with the pET plasmid. The pET plasmid contains kanamycin resistance gene, SUMO-tag, 6x His tag and a multiple cloning site as shown in Figure 2.7.

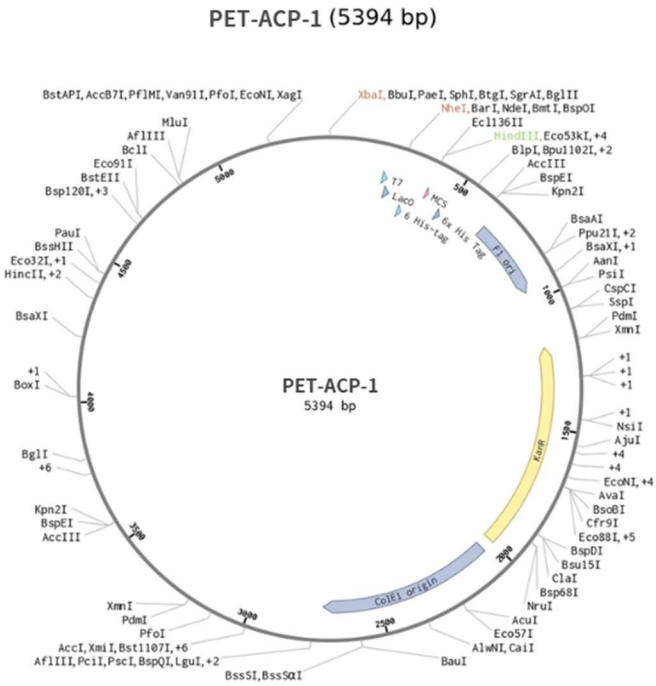

Figure 2.7 - Overview of plasmid design with insert ACP-1

2.5.1 Multiple Cloning Site

In our plasmid design, 2 cut sites, NdeI and SacI, located before and after SUMO are used to remove the SUMO part and insert the fusion peptide with cell-penetrating peptide (CPP). NheI is retained for further modification at 5' end if needed (Figure 2.8). KpnI is located in pET-plasmid after SacI for the 3' end modification if necessary.

Figure 2.8 - initial location of SUMO

2.5.2 6-His tag

It is one of the simplest and most widely used purification tags and commonly used in the production of recombinant proteins (Figure 2.9). These residues readily coordinate with transition metal ions immobilized on beads or a resin for purification.

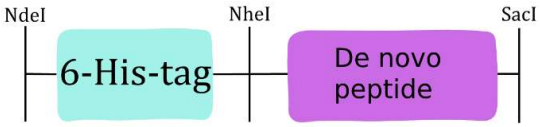

Figure 2.9 - Fusion peptide (*de novo* peptide) insert design

2.6 Cloning and Protein Expression

2.6.1 Digestion, ligation and transformation

SacI and NdeI were used to cut open the pET plasmid and also five fusion peptides (ACP1, ACP5, ACP7, ACP11 and ACP12), and then both insert and pET plasmid fragments would be ligated. The recombinant plasmid was transformed into DH5-alpha for cloning. And then, the plasmid was transformed into BL21 after the Colony PCR.

2.6.2 Colony PCR

To confirm whether the bacteria in the colony got the correct plasmid, colony PCR was conducted. We designed some primers for colony PCR. Details are shown in Table 2.5.

Table 2.5 - Sequence of primers for colony PCR

PRIMER NAME	ACCOMPLISHMENTS	Length(bp)
Primer (forward):	CGAAGTGGCGAGCCCGATCTTC	22
Primer (reverse):	GGCGAACGTGGCGAGAAAGGAA	22

2.6.3 Protein expression of de novo peptides

The constructed expression vector of the fusion peptide was inserted into BL21 for expression. A single colony was picked up and incubated in 20ml LB broth containing kanamycin(1X) at 37°C

with 150rpm shaking overnight. A total of 6ml incubated cell culture was then incubated into 240ml LB broth containing kanamycin (1X) at 37°C with 150rpm shaking until the OD600 reached 0.6. Then, 0.4mM IPTG was used to induce the protein expression for 24hrs at 20°C. And then, the cells were harvested by centrifugation at 6000xg for 20mins. The supernatant was collected. Then, 1ml lysis buffer with 1mM PMSF per 10ml culture was used to resuspend the pellet. Suspension was sonicated on ice (Amplitude: 95%; Time 5 min; Pulse 2s on, 2s off). It was cleared by centrifugation at 15000 rpm, 4°C for 15 mins.

2.6.4 Purification of de novo peptides

Both the sonicated suspension and the supernatant collected were purified by His-tag purification. After that, SDS-PAGE will be conducted to confirm whether the expression was induced successfully and the fusion peptides were purified. Afterwards, the concentration of products would be measured by Nanodrop.

2.6.5 Increase concentration of protein

To increase the concentration of the peptide, the Amicon Ultra-0.5 mL Centrifugal Filters for Protein Purification and Concentration is used. 500 µL of samples were added to the Amicon Ultra filter device, which is then placed into the centrifuge rotor. The device was spun at 14,000xg for 20mins. After that, the assembled device was removed from the centrifuge and the Amicon Ultra filter device was separated from the microcentrifuge tube. To recover the concentrated solute, the Amicon Ultra filter device was placed upside down in a clean microcentrifuge tube and placed in centrifuge. To transfer the concentrated sample from the device to the tube, it is spun for 2 minutes at 1,000xg. And then, the concentration of concentrated fusion peptide product would be measured by Nanodrop.

2.6.6 Molecular docking of the expressed fusion peptide with PDEδ

The expressed version of fusion peptides includes the His-tag and the related sequence. The amino acid sequences of the expressed fusion peptide are summarized in Table 2.6.

Table 2.6 - Amino acid sequences of the expressed fusion peptide (His-tag and the related sequence is labelled blue)

Expressed	Sequence
ACP1	MGSSHHHHHHGSGLVPRGSASSHISAVGPAAFTAEEIAESLGGSGGGSGRRRRRRRR
ACP5	MGSSHHHHHHGSGLVPRGSASAAAALAAALRALLQALAALQGGSGGGSGRRRRRRRR
ACP7	MGSSHHHHHHGSGLVPRGSASMPKVTVNSALAAAGAGHFGKGGSGGGSGRRRRRRRR
ACP11	MGSSHHHHHHGSGLVPRGSASMELKISGSEKSELMEELEKEGGSGGGSGRRRRRRRR
ACP12	MGSSHHHHHHGSGLVPRGSASATVPAPPKIDKAAQLASAAKGGSGGGSGRRRRRRRR

The amino acid sequence of the expressed version of ACP5 (KAPI) is used for further analysis in the ODE model constructed. The content is discussed in Appendix I (ODE Model). The predicted binding of ACP5 and PDEδ is shown in Figure 2.10. The calculated cLDDT and binding affinity is 0.294 and 8.638 respectively. It is shown that the addition of the His-tag and the related sequence hasn't affect the strong binding of ACP5 to PDEδ.

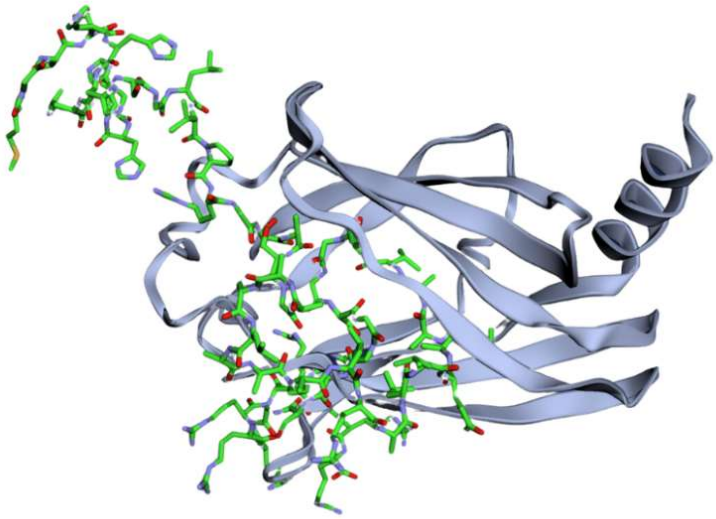

Figure 2.10 - Peptide ligand (Expressed version of ACP5)
binding with PDEδ visualized in DynamicBind

2.7 Cell Culture and Cytotoxicity Test

2.7.1 Cell passaging and cell seeding

The human epithelial lung cancer cell line A549 was purchased from the American Type Culture Collection (ATCC, USA). A549 were cultured in Dulbecco's Modified Eagle Medium F12/DMEM medium (Thermo Fisher Scientific, USA). A549 cells were cultured and seeded on a T75 flask at a density of $2.1x10^6$ cells. The previous culture medium was removed. TrypLE Express Enzyme (Thermo Fisher Scientific, USA) was added and cells were incubated in a CO_2 incubator until all adherent cells were removed from the lower surface of the plate. Transfer the content to a falcon tube and centrifuge it at 1000 rpm for 5 minutes. The supernatant was removed, while the cell pellet was then resuspended by fresh culture medium.

For cell counting, 10µl cell suspension and 10µl Trypan blue solution was mixed well. The mixture is loaded onto a hemocytometer and observed with EVOS XL Core Imaging System (Thermo Fisher Scientific, USA) to count the number of cells in four grids. The desired cell seeding density is 5000 cells per well. The required amount of cell suspension was mixed with the corresponding volume of culture medium in a falcon tube. The mixture was added into a reagent reservoir and transferred to the 96-well plate to perform cell seeding. The outer wells were filled with 200µl sterilized water to avoid disturbance of cells by excessive evaporation [25].

2.7.2 Drug treatment and measurement of cancer cell viability

After two days of growth, the previous growth medium was removed and cells were treated with new medium containing different concentrations of drugs. After the drug incubation, 10µl of CCK-8 reagent was added directly to the wells. The plates were then incubated for a specified period, within 30 minutes to one and a half hours, to allow sufficient time for the color to develop. After incubation, the absorbance of each well was recorded using a microplate reader with a wavelength of 450 nm. Since the intensity of the color is proportional to the number of viable cells, the cell viability of cancer cells treated with different concentrations of drugs can be compared.
In the measurement that involved 3D spheroid, 100µl of medium was removed and 10µl of CCK-8 reagent was added directly to the wells. The plate was shaken to ensure even distribution of newly formed formazan dye [26].

2.7.3 Effect of Cisplatin on cell line A549

Different concentrations (0, 1.56, 3.13, 6.25, 12.5 and 25μM) of Cisplatin were applied to A549 cell line to investigate their effect on cancer cell viability.

2.7.4 Effect of fusion peptides ACP1 and ACP5 on A549

Different concentrations (0, 25 and 50μM) of the fusion peptide were applied to A549 cell line to investigate their effect on cancer cell viability.

2.7.5 Further cytotoxicity test of ACP5 (KAPI) for A549

Different concentrations (0, 1.56, 3.13, 6.25, 12.5, 25 and 50μM) of KAPI were applied to A549 cell line to investigate their effect on cancer cell viability.

2.7.6 Cytotoxicity test of KAPI for BEAS-2B

Different concentrations (0, 25 and 50μM) of KAPI were applied to BEAS-2B cell line (normal human bronchial epithelium) to investigate their effect on normal cell viability.

2.7.7 Combination effect of KAPI and Cisplatin

The combination effect of KAPI and Cisplatin (Table 2.7) to A549 cell line was studied.

Table 2.7 - Summary of the combination effect of the most efficiency ACP (KAPI) and Cisplatin treatment conducted on cell line A549

KAPI concentration in culture medium (µM)	Cisplatin concentration in culture medium (µM)				
0	1.56	3.13	6.25	12.5	25
25					
50					

2.8 Drug screening by Multi-Cellular Tumor Spheroid (MCTS)

2.8.1 3D cell seeding

Multi-Cellular Tumor Spheroid (MCTS) was grown with 100µl of cell suspension per well by transferring to a U-bottom 96-well Nunclon Sphera microplates (Thermo Fisher Scientific) [27]. The plate was centrifuged at 2500 rpm for 5 minutes [28] to help the cells clump at the bottom of the well and facilitating uniform spheroid formation (Figure 2.11).

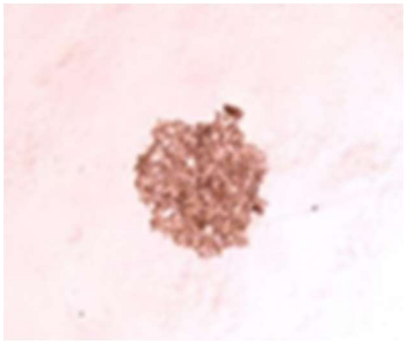

Figure 2.11 - Cell clump at the bottom of the well

2.8.2 Analysis of spheroid growth

Achieving consistent and reproducible spheroid sizes and shapes can be challenging, which is crucial for experimental reliability. To maintain consistency in the spheroids selected for the analysis of cancer growth, tier 1 and tier 2 screenings are conducted. In tier 1 screening, the morphology and sphericity of the spheroid were assessed via live imaging using the inverted microscope. The sphericity of the spheroids was assessed and those with low sphericity (Figure 2.12) were excluded from the downstream processing. After tier 1 screening, the spheroids with a similar morphology proceeded to tier 2 screening.

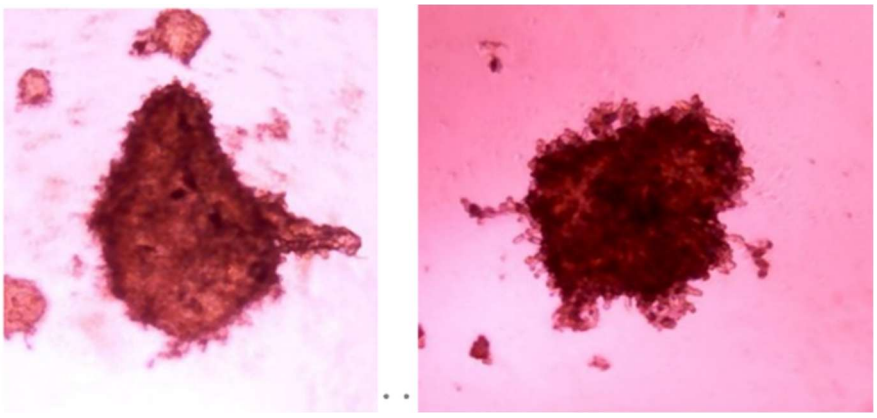

Figure 2.12 - Spheroids with low sphericity

In the tier 2 screening, the software tools ImageJ and ReVISP were employed to assess their diameter and volume, respectively. [29] Through capturing an image of hemocytometer under 4X microscope, diameter of spheroid was measured with ImageJ. (Figure 2.13 and 2.14)

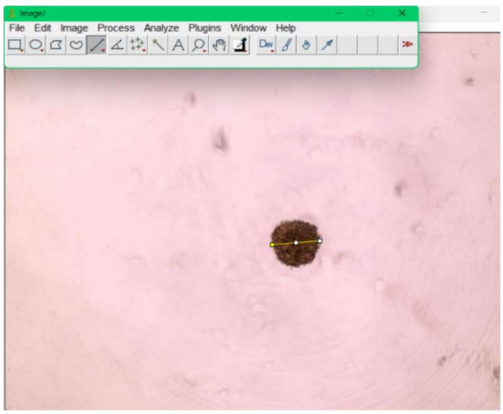

Figure 2.13 - Measurement using ImageJ

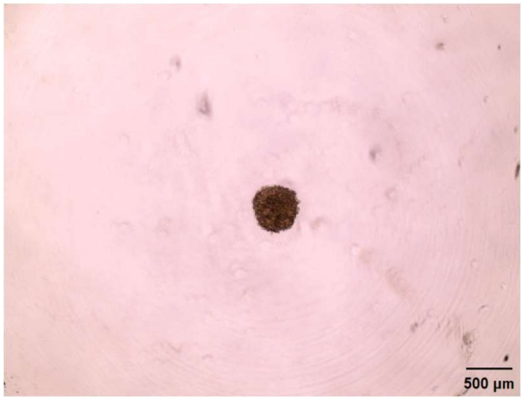

Figure 2.14 - Diameter of spheroid shown with scale bar

Next, the volume of the spheroid was estimated by ReVISP by reconstructing the 3D shape of multicellular spheroids and for the estimation of volume by counting the voxels (3D pixels) fully included in the 3D surface [30], [31]. (Figure 2.15).

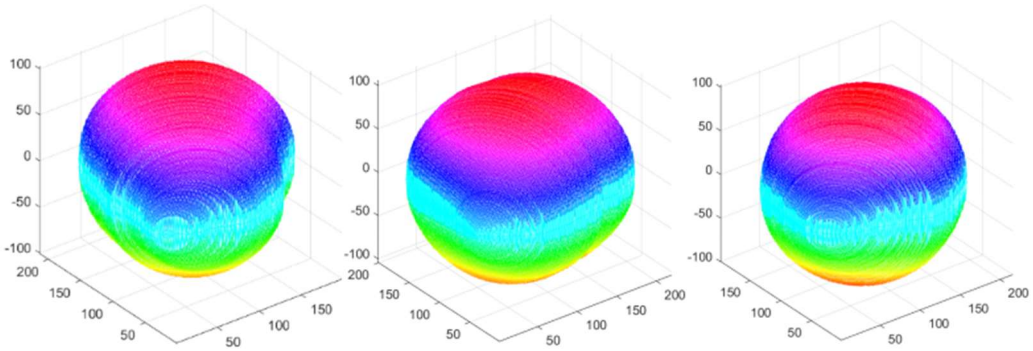

Figure 2.15 - The 3D estimation of spheroid shape by ReVISP

The data diameter and volume of each spheroid is obtained. Coefficient of variation (CV) was calculated to assess the reliability of the data obtained. CV value is a measure of precision and is equal to the standard deviation quantity divided by the mean quantity of a group of replicates. CV is commonly used to assess the reproducibility of in vitro models, and CV scores of <20% variation are considered acceptable. Also, spheroids' data beyond 2 SDs from the mean are considered outliers. Those will be excluded from downstream processing. In conclusion, through tier 1 screening and the application of ImageJ and REVISP, consistent spheroid size and uniformity can be maintained for more precise measurement in cytotoxicity test. (Figure 2.16)

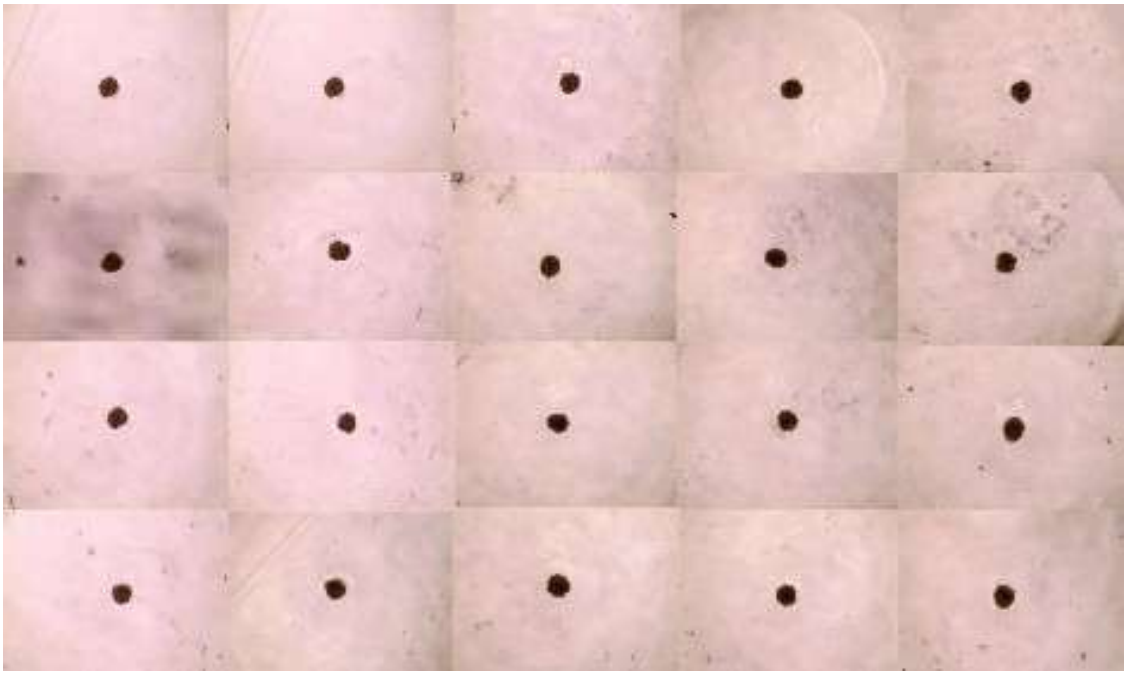

Figure 2.16 - Consistent spheroid size and uniformity was maintained for further analysis

2.8.3 Effect of Cisplatin on cell line A549 (3D)

Different concentrations (0, 1.56, 3.13, 6.25, 12.5 and 25μM) of Cisplatin were applied to 3D MCTS of A549 cell line to investigate their effect on cancer cell viability.

2.8.4 Effect of ACP5 (KAPI) on cell line A549 (3D)

Different concentrations (0, 1.56, 3.13, 6.25, 12.5, 25 and 50μM) of ACP5 (KAPI) were applied to 3D MCTS of A549 to investigate their effect on cancer tumour viability.

2.9 Proof concept - qPCR Essay

To verify the molecular mechanism of KAPI, reverse transcription and quantitative PCR (qPCR) was carried out. Cells were seeded at a 6-well plate with a density of 0.3 x 10^6 cell per well. After two days of cell growth, the old medium was removed and the new medium with 0μM, 25μM and 50μM ACP5 (KAPI), were added into the well respectively. After treatment for 4 hours, TRIzol (Biosharp Life Sciences) was used to extract total RNA of different treated group. The absorbance values at wavelengths of 260 and 280 nm of the total RNA were measured by Nano-Drop ND-1000 spectrophotometry, and the OD260/OD280 ratio was calculated to make sure the RNA sample is of good quality (ratio >1.80).

The gene expression levels of EGFR1, BRAF, Pl3K were checked, with GAPDH2 as housing keeping gene. The primer sequences (synthesized by BGI Tech Solutions) were shown in Table 2.8.

Table 2.8 - List of primers used in qPCR

	Target	Sequence (Fwd)	Sequence (Rev)
KRAS upstream	EGFR [32]	AACACCCTGGTCTGGAAGTACG	TCGTTGGACAGCCTTCAAGACC
	SOS [33]	GGAGATCAACCCTTGAGTGCAG	TGCTCTACCCAGTGCCGACATA
Pl3K/ARK/mTOR pathway	Pl3K [34]	ATGCCAGAAAGGAGAATG	TGTTGGACTCAGCAATAC
MARK/ERK pathway	BRAF [32]	TCATAATGCTTGCTCTGATAGGA	GGCCAAAAATTTAATCAGTGGA
Housekeeping gene	GAPDH	AGCCACATCGCTCAGACA	TGGACTCCACGACGTACT

Ct value obtained in each sample was normalized to its reference level as ΔCt= Ct (signalling pathway gene)-Ct (house-keeping gene). The Ct value was the quantification cycle number and ΔΔCt was the difference of ΔCt (samples) with the ΔCt (control, KAPI=0μM). The reduction of mRNA level was expressed as a percentage and calculated with the formula (2^-ΔΔCt).

3. Results

3.1 Cloning and Protein Expression

3.1.1 Digestion, ligation and transformation

SacI and NdeI were used to cut open the pET plasmid and also the sequence for the five fusion peptides (ACP1, ACP5, ACP7, ACP11 and ACP12), and then both insert and fragments were ligated. The diagrams below show that all inserts carried by the non-expression plasmid were successfully digested by SacI and NdeI. Target bands were observed, so all target genes were cut successfully as shown in Figures 3.1 to 3.3.

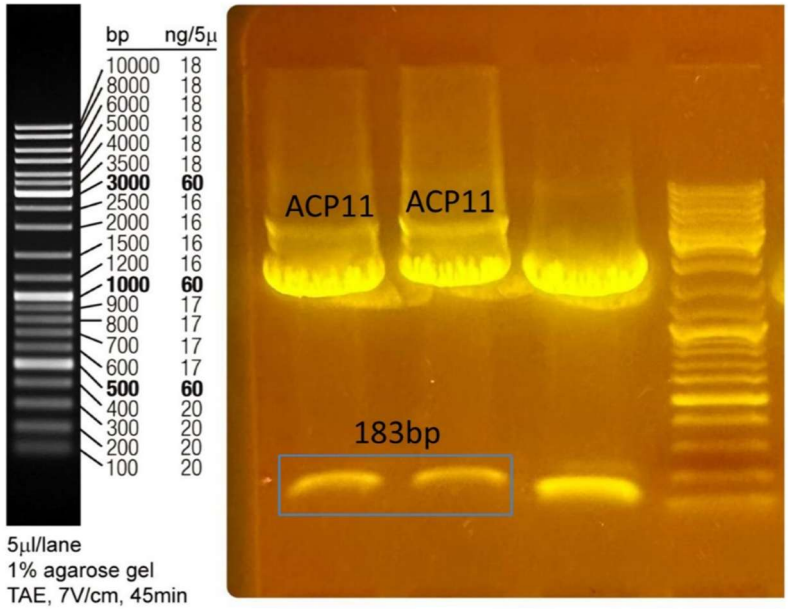

Figure 3.1- Result of digested product of ACP11 with plasmid

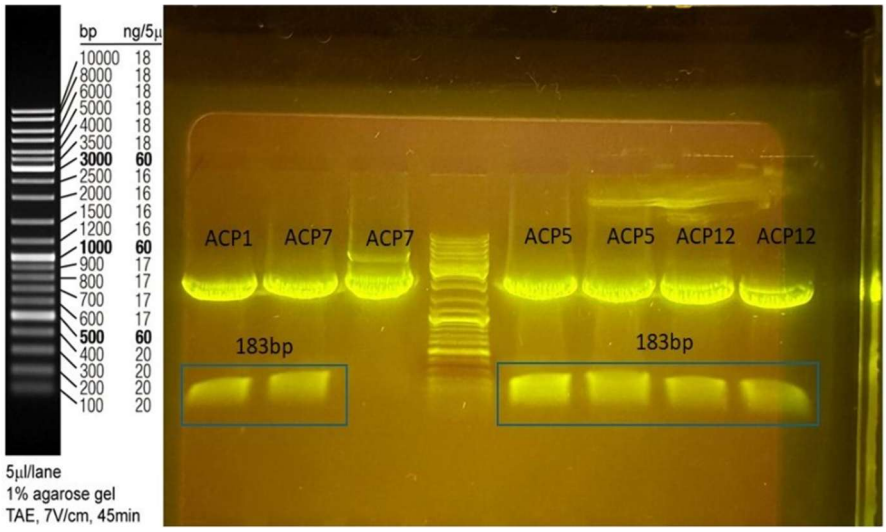

Figure 3.2 - Result of digested products of ACP1, ACP5, ACP7 and ACP12 with plasmid

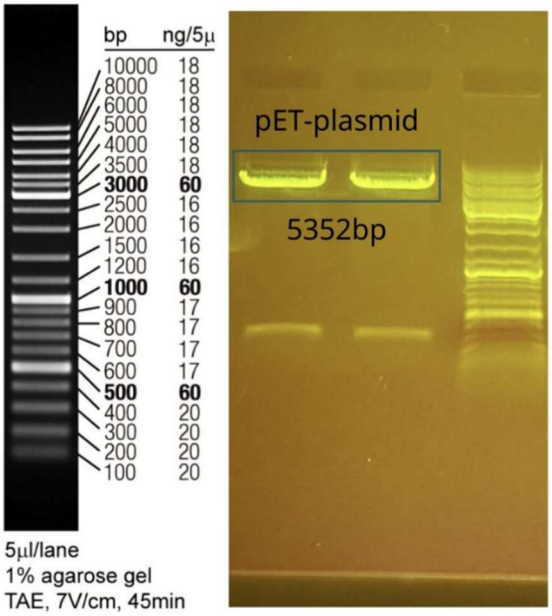

Figure 3.3 - Results of digested product of pET- SUMO plasmid

3.1.2 Colony PCR

Totally, 5 recombinant plasmids were transformed into DH5-alpha and colonies were observed in LB plate with kanamycin. Colony PCR was carried out. Only ACP1 and ACP5 got positive results in some colonies (Figures 3.4 and 3.5).

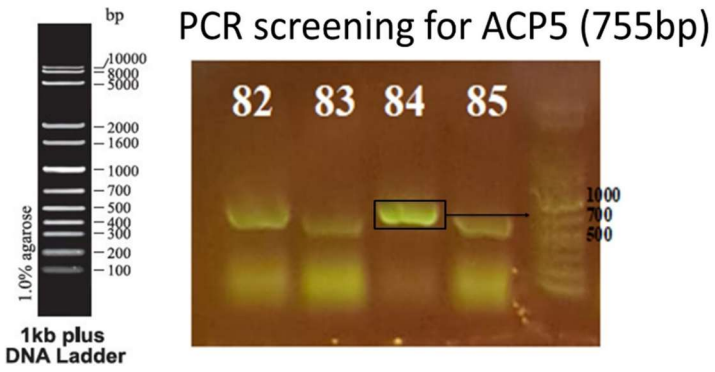

Figure 3.4 - The results of colony PCR of ACP5

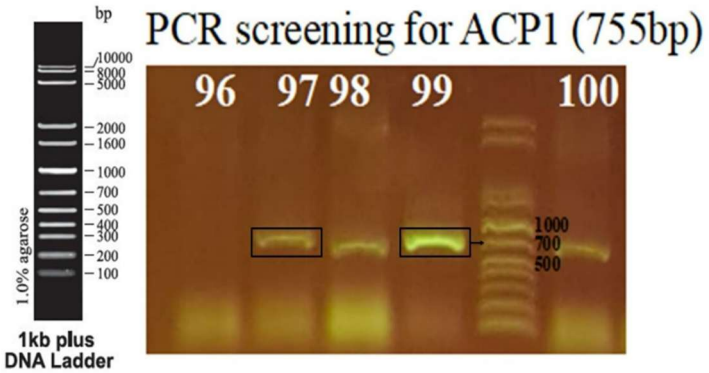

Figure 3.5 - The results of colony PCR of ACP1

3.1.3 Protein production and purification

The suspensions of both peptides were purified by Ni-NTA resin and eluted in PBS. This step was repeated three times. And then, SDS-PAGE was conducted to confirm whether purification succeeded. Protein bands at about 3-6kDa were observed in elution for ACP1 and ACP5 before and after purification. Measured by nanodrop, the concentration of ACP1 and ACP5 is 0.4360 µg/ µl and 0.4215 µg/ µl respectively.

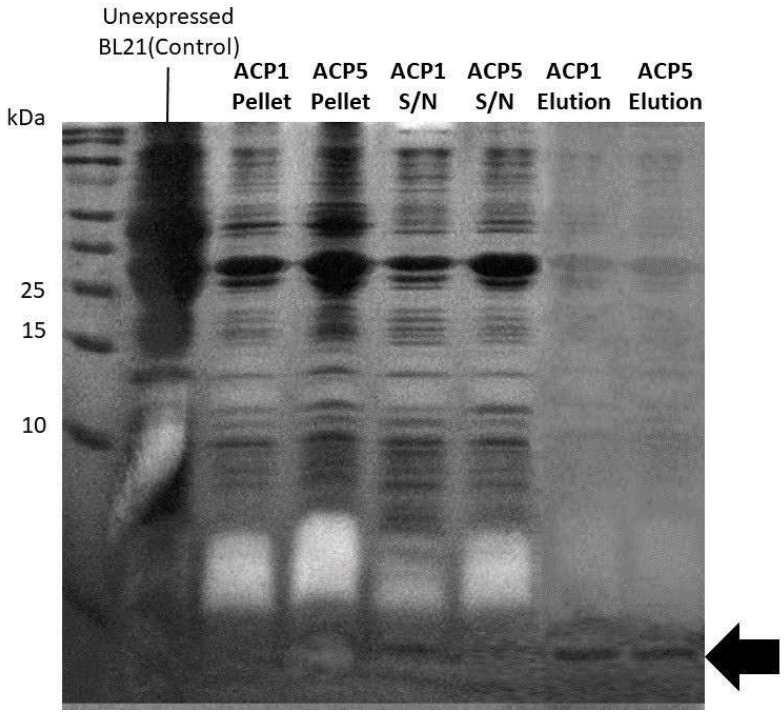

Figure 3.6 - The results of SDS-PAGE of ACP1 and ACP5 purification

3.1.4 Concentrating the peptides

To increase the concentration of the peptide, the Amicon Ultra-0.5 mL Centrifugal Filters were used for protein purification and concentration. Below table shows the concentration of each peptide before and after concentration.

Table 3.2 - Concentration of different ACP peptides after 1st and 2nd concentration

Concentration (µg/µl)		ACP1	ACP5
	Original	0.4360	0.4215
	After concentration	7.0196	6.9126

3.2 Cell Culture and Cytotoxicity Test

3.2.1 Drug screening of Cisplatin for A549

To find out whether A549 is particularly sensitive or resistant to cancer drug, the effect of Cisplatin on the cell line was tested. The results were shown in Figure 3.7.

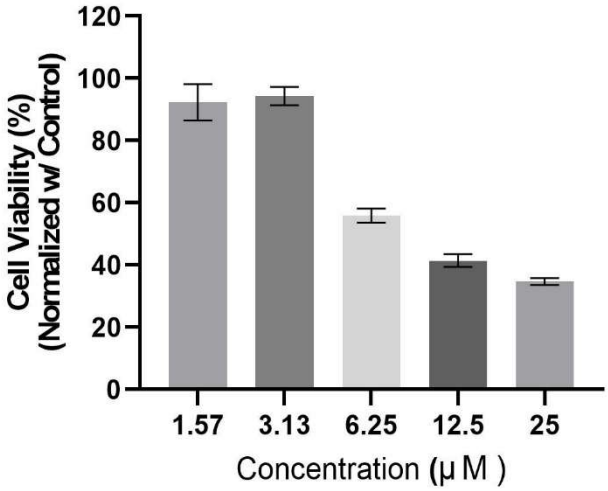

Figure 3.7 - Cell viability of A549 under different concentration of cisplatin

3.2.2 Drug screening of ACP1, ACP5 for A549

The effect of ACP1 and ACP5 on A549 cell line were tested. A549 cells were treated with ACP1 and ACP5 with concentrations of 0μM, 25μM, 50μM and respectively. The results were shown in Figure 3.8.

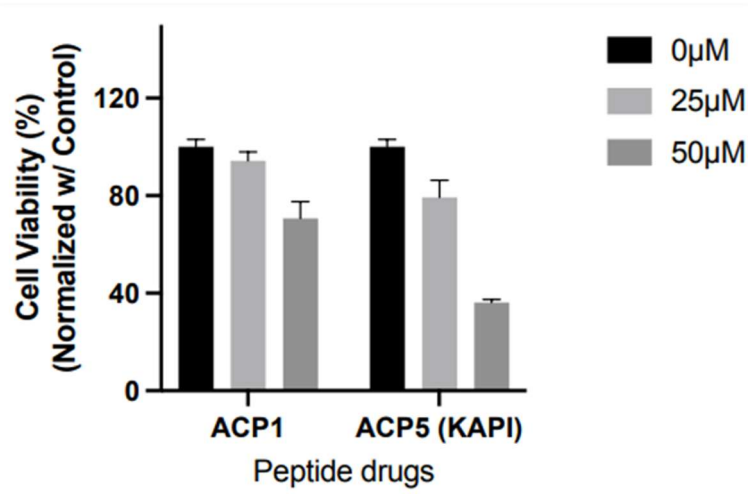

Figure 3.8 - Cell viability of A549 under different peptide drug treatments at various concentrations

3.2.3 Further cytotoxicity test of ACP5 (KAPI) for A549

The effect of ACP5 on A549 cell line was further tested. A549 cells were treated with ACP5 with different concentrations. The results were shown in Figure 3.9.

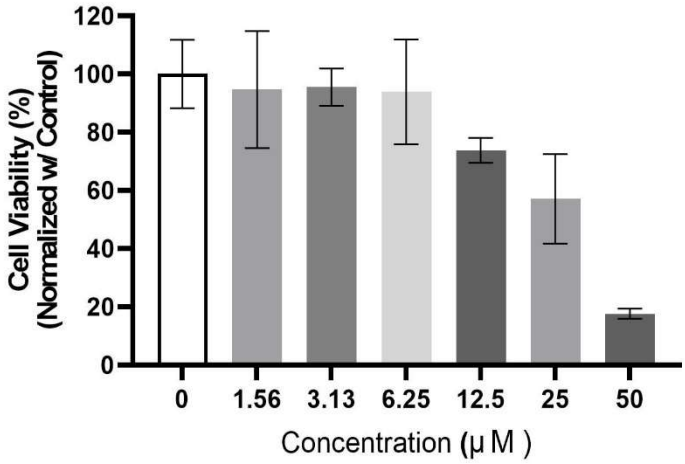

Figure 3.9 - Cell viability of A549 under different concentration of KAPI

3.2.4 Cytotoxicity test of ACP5 (KAPI) for BEAS-2B

The effect of ACP5 on BEAS-2B cell line was tested. The results were shown in Figure 3.10.

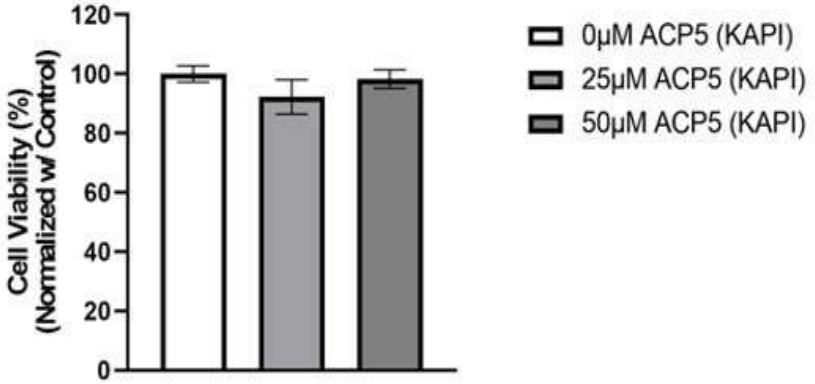

Figure 3.10 - Cytotoxicity test of ACP5 (KAPI) on cell line BEAS-2B

3.2.5 Combination effect of KAPI and Cisplatin

The combination effect of KAPI and Cisplatin on A549 cell line was tested. The results were shown in Figure 3.11.

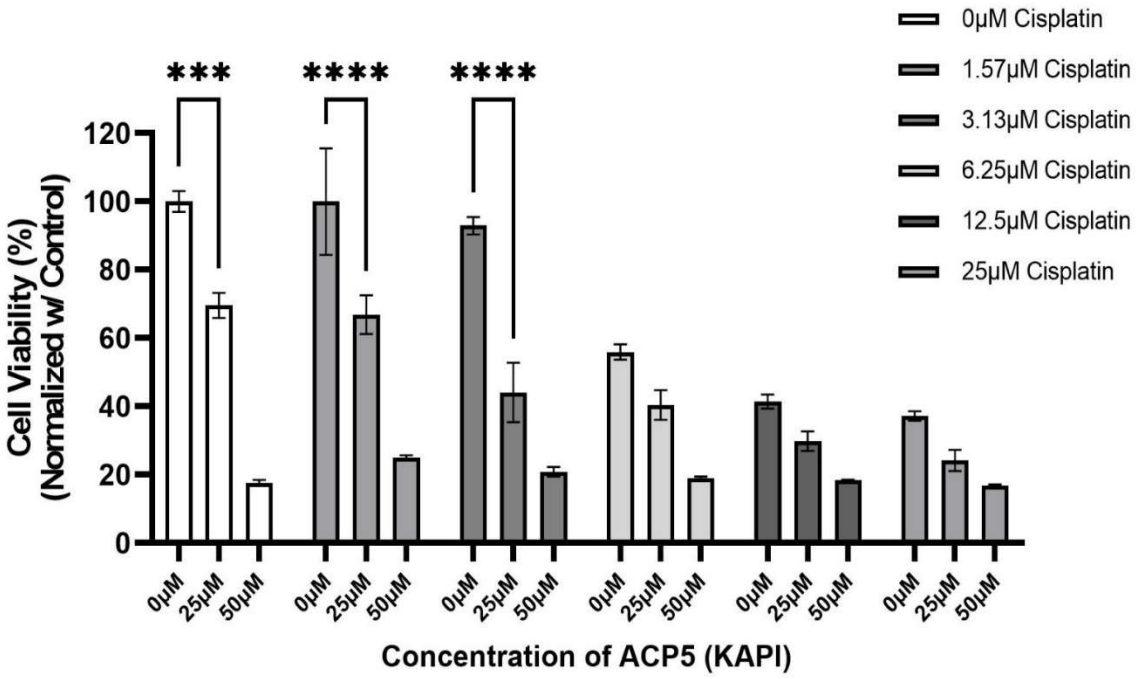

Figure 3.11 - The combination effect of ACP5 (KAPI) and Cisplatin on the cancer cell viability

3.2.6 Effect of Cisplatin on cell line A549 (3D)

The effect of Cisplatin on A549 (3D MCTS) was analyzed. The results were compared with that in 2D culture and shown in Figures 3.12.

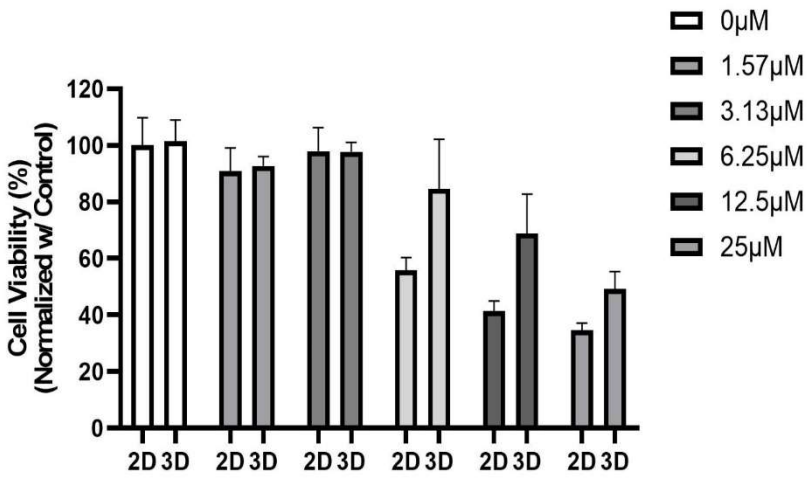

Figure 3.12 - Cell viability of A549 cells (2D) and MCTS (3D) under different concentration of Cisplatin

3.2.7 Effect of ACP5 (KAPI) on cell line A549 (3D)

The effect of ACP5 (KAPI) on A549 (3D MCTS) was analyzed. The results were shown in Figures 3.13.

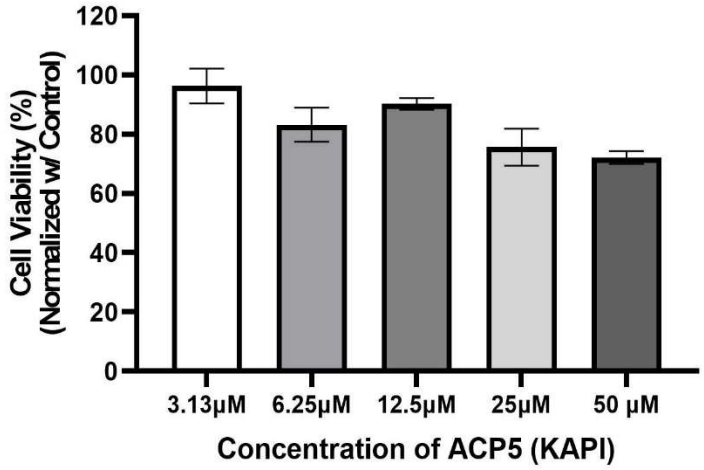

Figure 3.13 - Tumour viability under various concentrations of ACP5 (KAPI)

3.3 Proof concept - qPCR Essay

To understand the impact of KAPI on gene expression involved in the KRAS pathway, quantitative PCR (qPCR) was conducted to measure the expression levels of SOS1, EGFR, PI3K, and BRAF in A549 cells treated with 50μM KAPI, compared to untreated cells. Fold change of various genes after the normalization with GAPDH were shown in Figure 3.14.

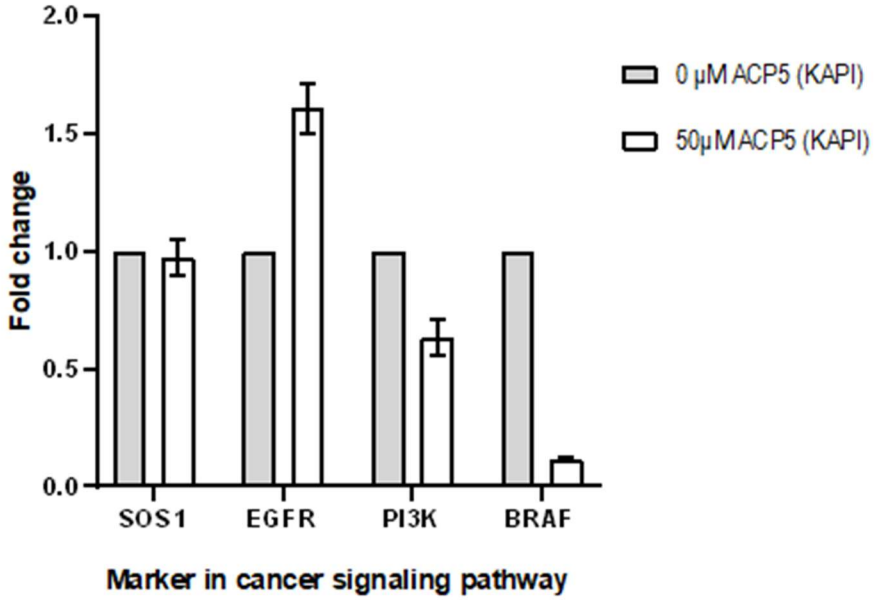

Figure 3.14 - Fold change of four markers in the cancer signalling pathway

4. Discussion

4.1 Cell Culture and Cytotoxicity Test

4.1.1 Drug screening of Cisplatin for A549

Cisplatin does not have significant effect on the cell viability of the A549 cancer cells with concentrations between 1.56μM and 3.13μM (Figure 3.7). However, cell viability showed an apparent decline when the concentration of Cisplatin continues to increase.

The IC50 value is estimated to be 5.33μM, [35] which is close to 6.14μM, as determined by other related research on cell line A549. [36] It shows that the cell line used is not particularly vulnerable to cancer drug.

4.1.2 Drug screening of ACP1, ACP5 for A549

At concentration of 50μM, only ACP5 (KAPI) has significant effect compared to the control (Figure 3.8). The anti-cancer abilities of ACP5 (KAPI) are much higher than ACP1. At concentration of 50μM, KAPI's inhibition on cell viability on A549 is approximately 80%. This showed that ACP5 (KAPI) was more effective in anti-cancer ability as compared with ACP1.

4.1.3 Further cytotoxicity test of ACP5 (KAPI) for A549

The dosage response of A549 to KAPI was assessed (n=3). According to the results (Figure 3.9), KAPI has little effect on the cell viability of the A549 cancer cells with concentrations between 1.56μM and 6.25μM. However, cell viability showed an apparent decline when the concentration was increased to 12.5μM, 25μM and 50μM with cell viability of approximately 70%, 55% and 18% respectively. The IC50 of KAPI is determined to be 25.9μM.

4.1.4 Cytotoxicity test of ACP5 (KAPI) for BEAS-2B

The cytotoxicity test was conducted with the fusion peptide ACP5 (KAPI) on cell line BEAS-2B (n=3). BEAS-2B, which is a non-cancerous bronchial epithelial cell line, served as a control to investigate the effect of the peptide drugs on non-cancerous human cells. [37] According to the results (Figure 3.10), it has been shown that ACP5 (KAPI) has a limited effect on the growth of the BEAS-2B cell line. This finding suggested that ACP5 (KAPI) does not alter the proliferation as well as viability of A549 on a large scale. The limited effect on BEAS-2B cells indicates that ACP5 (KAPI) may have a favorable safety profile, as it does not adversely affect this type of healthy cells.

4.1.5 The combination effect of KAPI and Cisplatin

As indicated (Figure 3.11), as 25μM or 50μM of ACP5 (KAPI) is introduced with Cisplatin, the percentage inhibition of cell viability is enhanced, as compared with the same concentration of Cisplatin. In addition, it is shown that 12.5μM of Cisplatin with 0μM ACP5 (KAPI) showed a similar degree of inhibition as 6.25μM with 25μM of ACP5 (KAPI).

Cisplatin is one of the most used chemotherapy drugs. It is estimated that 10% to 20% of all cancer patients use Cisplatin and other similar platinum-based drugs. [38] Cisplatin is a highly effective anticancer drug used to treat various cancers. However, its clinical use is limited due to severe side effects, ranging from nephrotoxicity, neurotoxicity and ototoxicity. These effects are always cumulative and dose dependent. Between 20% and 35% of patients experience acute kidney injury (AKI) following Cisplatin treatment and there is no clinically effective drug to prevent or treat Cisplatin-induced nephrotoxicity.[39] Acute kidney injury with repeating episodes can result in impaired renal tubular function, acute renal failure, chronic kidney disease, uremia, and hypertensive nephropathy. [40] Meanwhile, it is demonstrated that ACP5 (KAPI) has a good potential in reducing the required dosage of Cisplatin in combination therapy so as to minimize those side effect of Cisplatin in chemotherapy.

4.1.6 Effect of Cisplatin on cell line A549 (3D)

In both 2D and 3D (MCTS) culture, cell viability decreases as the concentration of Cisplatin increases, indicating that higher concentrations of the substance reduce tumour viability (Figure 3.12). However, 3D MCTS culture showed an enhanced resistance towards the effect of Cisplatin. As the concentration increases, the difference in cell viability between 2D and 3D conditions becomes more pronounced, with 3D cultures generally showing higher viability than 2D cultures at the same concentrations. It can be explained by the reduced surface area to volume ratio in the 3D MCTS culture compared to that in 2D culture.

4.1.7 Effect of ACP5 (KAPI) on cell line A549 (3D)

In assessing the effectiveness of ACP5 (KAPI) on tumour viability (Figure 3.13), it is shown that tumour viability is reduced by 20% after a two-day treatment. The dense structure of 3D spheroids can limit the penetration of drugs, resulting in lower drug concentrations reaching the inner cells.

4.2 Proof of concept - qPCR Essay

As the proof of KAPI's proposed mechanism, the result of qPCR was interpreted. Firstly, SOS facilitates the exchange of GDP for GTP on RAS proteins, converting them from an inactive to an active state. This activation is essential for transmitting signals from cell surface receptors to the nucleus, promoting cell proliferation and survival. [41] The expression level of SOS remains relatively unchanged (fold change close to 1), indicating that KAPI treatment does not significantly affect SOS mRNA levels. This suggests that SOS may not be a primary target of KAPI or that its regulation is not directly influenced by PDE delta inhibition.

Next, EGFR expression is upregulated by approximately 52% in response to KAPI treatment. This increase could be a compensatory mechanism where cells attempt to maintain signaling through the EGFR pathway despite the inhibition of KRAS signaling. EGFR upregulation might also indicate feedback activation as a response to disrupted downstream signaling in KRAS. [41]

For PI3K, its expression is reduced by approximately 37% with 50μM KAPI treatment. This downregulation suggests that KAPI effectively inhibits the PI3K pathway, which is a critical downstream effector of KRAS signaling. Reduced PI3K levels indicate a successful disruption of the signaling cascade, potentially leading to decreased cell proliferation and survival. [42]

Similarly, BRAF expression is significantly downregulated (approximately 89% reduction) in response to 50μM KAPI treatment. This substantial decrease indicates that BRAF, another key downstream effector of KRAS, is highly sensitive to PDE delta inhibition by KAPI. The marked reduction in BRAF levels suggests a strong inhibitory effect on the MAPK/ERK pathway, which is crucial for cell growth and survival. [43]

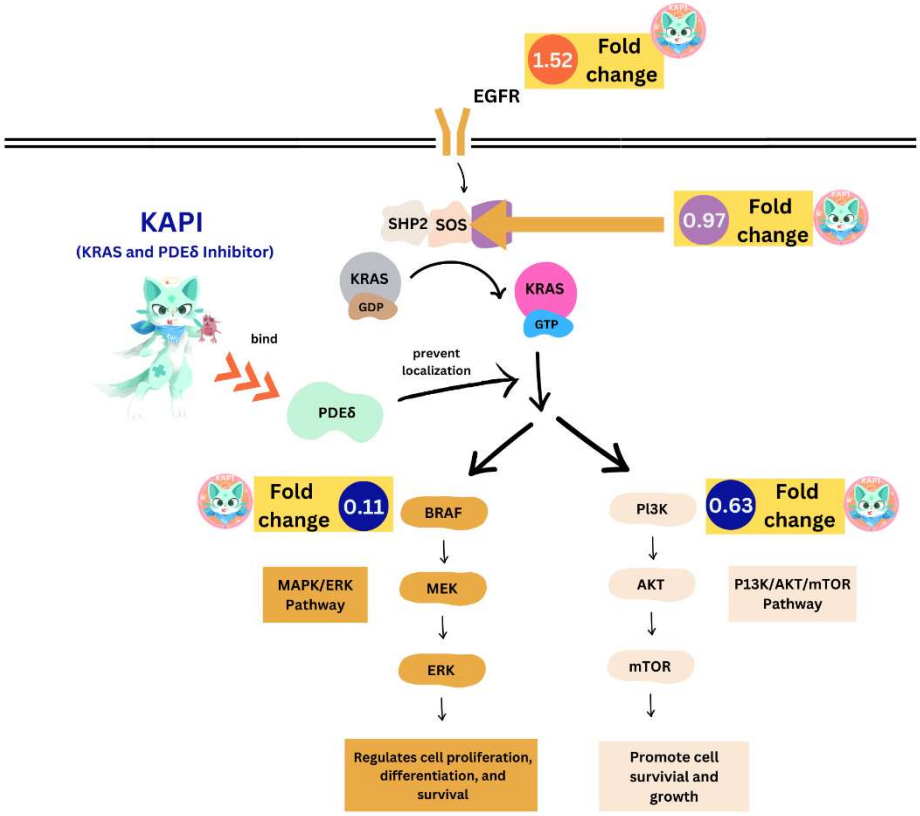

Figure 4.1 - Regulation of PDE delta related expression

In conclusion, the qPCR results demonstrate that KAPI effectively modulates the expression of key genes in the KRAS signaling pathway. The significant downregulation of PI3K and BRAF, along with the upregulation of EGFR, highlights the complex regulatory mechanisms and potential compensatory responses in cancer cells (Figure 4.1). These findings support the potential of KAPI as a therapeutic agent targeting PDE delta to inhibit KRAS-driven oncogenic signalling.

4.3 Application

Ways of administering KAPI as chemotherapy drug in cancer patients are discussed in this section. There are three proposed ways of applying KAPI to the human body: intravenous infusion, oral drug and mRNA therapeutics. In intravenous infusion, drug is injected directly into the venous system and the effect is rapid. Oral drugs provide a convenient approach to patients' treatment while some of the peptides may be lost in the digestion. [44] For mRNA therapeutics, it is more flexible and cost-effective than conventional approaches that may offer. [45] As a consequence, different methods are discussed in order to meet different people's needs and benefit a wider audience.

4.3.1 Intravenous infusion

4.3.1.1 Background

Like traditional chemotherapy e.g. Cisplatin, KAPI can be administered directly into the bloodstream through intravenous infusion. This method ensures rapid distribution throughout the body and the effect of the drug can be quick.

4.3.1.2 Challenges

A potential problem is that the drugs can have serious non-specific cardiopulmonary effects. [46] Hence, a high dosage of drugs is rarely used. Instead, drugs are injected over a period of time with a controlled pace. Also, the instability of the peptide suggests that it may degrade quickly under physiological conditions, potentially limiting its therapeutic efficacy. Next, the efficiency of the drug can be limited due to various physiological barriers, resulting in low permeability, and drug degradation. [47]

4.3.1.3 Recommendation

4.3.1.3.1 Cell penetrating peptide (CPP) approach

The CPPs approach is a promising strategy for enhancing the permeability of therapeutic proteins and peptides across cellular membranes, especially when oral administration is considered. In our project, KAPI's permeability for cell membranes is enhanced by the combining with polyarginine Cell-Penetrating Peptide (CPP), as discussed in section 2.3. A good example of this represents cell-penetrating peptide-based oral delivery of anti-diabetic therapeutics, including oral insulin. [48]

4.3.1.3.2 Optimize dosage by mathematical modeling

The challenge inspires us to develop an Ordinary Differential Equation (ODE) model to better understand and predict the peptide's behavior over time. By incorporating factors such as degradation rate, cancer growth rate, the ODE model will help us simulate and optimize the in-vitro chemotherapy treatment, facing challenge from peptide's stability and efficacy for potential therapeutic applications. The content is discussed in Appendix I - ODE Model.

4.3.2 Oral administration

4.3.2.1 Background

Oral administration is the most often used treatment for gastrointestinal cancer. The drug is absorbed along the gastrointestinal tract. Oral delivery has advantages over other forms of delivery which lead to better patient acceptability and reduce frequency and painless administration, which can help in better disease management. [47] It is more convenient to use, because it's small in size. Patients can self-administer oral drugs without the assistance from professionals. Next, it is more comfortable for patients, especially those who may have a fear of needles.

4.3.2.2 Challenges

Once administrated orally, KAPI faces a harsh environment of the gastrointestinal tract, which limits its bioavailability. The absorption of KAPI can be affected by the pH environment of the digestive tract. When KAPI pass through the stomach, a part of the drugs may be hydrolyzed and lose their biological activity due to the extreme pH environment. Consequently, the majority of KAPI may undergo rapid degradation in the stomach. [48], [49]

Besides, various proteolytic enzymes can lead to the degradation of drugs into small peptides or amino acids. [40] For example, pepsins in the stomach or pancreatic protease can lead to the inactivation of KAPI, which is peptide in nature. In the site of absorption, protease in intestinal juice can also break down peptides into amino acids. Therefore, the enzyme barrier in the digestive tract has become a major obstacle to the absorption of KAPI. [50]

4.3.2.2 Recommendation

4.3.2.1.1 Administration of KAPI in sodium alginate microsphere

To tackle the challenge from extreme pH, it is suggested that KAPI is administered in sodium alginate microsphere. Sodium alginate microsphere is chosen as KAPI's carrier because of its strength in enhanced bioavailability and controlled release of drug. KAPI is mixed well with soluble sodium alginate (Phygene Scientific) followed by drying to allow formation of microsphere. Hydration of an alginate matrix leads to the formation of a gelatinous layer which can act as a drug diffusion barrier. [51]

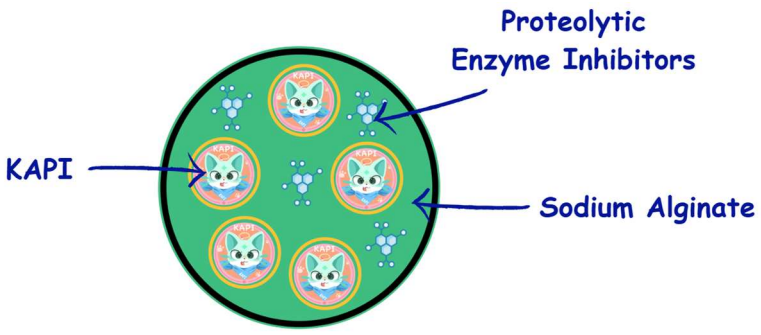

Figure 4.2 - The basic design of oral drugs

A simple experiment has been conducted to demonstrate that the microsphere can fit the needs of KAPI's oral administration. From the test, sodium alginate microspheres containing dye, quercetin, were added into simulated stomach acid (Phygene Scientific) and alkaline simulated intestinal fluid (Phygene Scientific). No dyes leak out in the simulated stomach acid while dyes leak out in the simulated intestinal fluid. This suggests that the dye in microsphere is not released in an acidic environment but only dissociated under a pH value similar to intestinal fluid. Therefore, it prevents KAPI from degrading in gastric juice and ensures KAPI be released into the small intestine for absorption so that KAPI can enter the bloodstream without losing its function. [51]

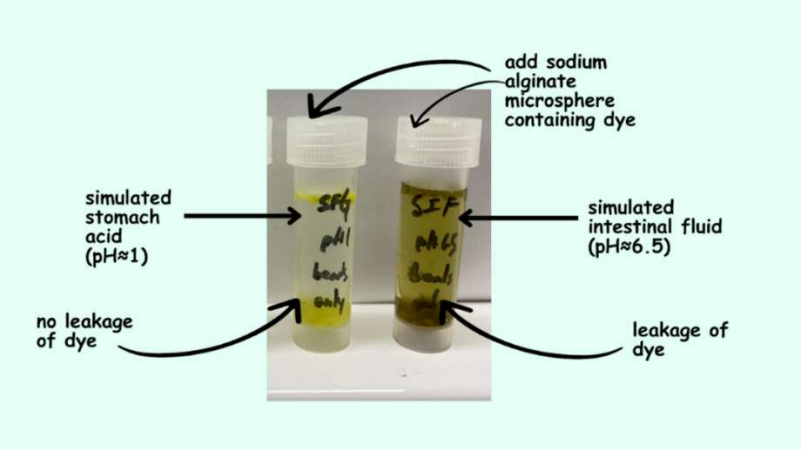

Figure 4.3 - A test of sodium alginate microspheres containing dye in two different pH

4.3.2.1.2 Administration of proteolytic enzyme inhibitor in the microsphere

To tackle the challenge from protease, it is suggested that proteolytic enzyme inhibitor is administered, together with KAPI, in sodium alginate microsphere. Protein and peptide drugs are easily degraded by various enzymes in the gastrointestinal tract. Therefore, enzyme inhibitors can effectively prevent enzymatic degradation of protein and peptide drugs and increase drug absorption. [49] Research shows that after oral application of enzyme inhibitors, the oral bioavailability of peptides drugs was significantly improved. Examples of inhibitors include a model proteolytic enzyme - aprotinin, which is a trypsin inhibitor. [52] Nevertheless, the inhibitor might result in increased secretion of pancreatic proteases in long-term treatment. [53]

4.3.3 mRNA therapeutics

4.3.3.1 Background

During the severe acute respiratory syndrome coronavirus 2 (SARS-CoV-2) pandemic, mRNA vaccines play a crucial role in controlling the spread of the disease. The mRNA-based approach can theoretically produce any protein/peptide via the protein synthesis machinery in the transfected cell in vivo. [54] Hence, with the mRNA therapeutics, cancer cells can produce KAPI on its own.

In vitro transcribed mRNA has achieved programmed production, which is more effective, faster in design and production. [45] Only RNA polymerase, nucleotides and DNA templates are needed.

The mass production of mRNA can be conducted in a self-free system, culturing and harvesting cells is not necessary, thus it saves significant time and cost. [44], [55]

4.3.3.2 Challenges

mRNA is highly susceptible to RNases. The half-life of direct intravenous administration of mRNA should be very short due to their susceptibility to degradation by nucleases. Hence, it is quite difficult for mRNA to pass through the anionic cell membrane and translate functional proteins in cancer cells. [56] Hence, additional barriers include high renal clearance, non-specific tissue distribution, and off-target effects. [57]

4.3.3.3 Recommendation

The application of novel drug delivery devices was considered as the most promising innovative pharmaceutical approaches in drug delivery systems. [58] Due to the susceptibility of IVT mRNA to degradation by nucleases, it is crucial to select an appropriate delivery vehicle to safeguard the integrity of the mRNA prior to its intracellular delivery. By Using IVT mRNA synthesis, we can produce a substantial amount of mRNA in vitro. This mRNA can be encapsulated in liposome, which protects it, aids in injection, and maintains its stability. The liposome shields the mRNA from degradation and assists in delivering it to target cells, where it is translated into KAPI. This process enables the body to produce KAPI independently, ensuring prolonged expression of KAPI for extended clinical benefits. [55], [59], [60]

4.3.4 Comparison with existing chemotherapy option

Chemotherapy has long been a cornerstone in the treatment of various cancers, offering a range of drugs that target rapidly dividing cells. However, the landscape of chemotherapy is continually evolving, with new agents and combinations being developed to enhance efficacy and reduce side effects. This comparison aims to evaluate the advantages and limitations of our invention: KAPI in the context of existing chemotherapy options.

According to our search in Google Patent, cancer drug's targets are diversified. We have compared traditional chemotherapy drug Cisplatin (Google Patent: US4310515A), KRAS G12C Inhibitor (Sotorasib)(Google Patent: US 2024/0139193 A1) and Pembrolizumab (Google Patent: LU92940I2). The content is discussed below:

Table 4.1 Comparison with Cisplatin

Cisplatin	
Description	Cisplatin is a platinum-based chemotherapy drug that works by interfering with the DNA of cancer cells, ultimately leading to their death. Binding of Cisplatin with DNA prevent the DNA from unwinding and replicating properly, thereby inhibiting DNA synthesis and transcription. This disruption triggers a series of cellular responses, including the activation of DNA repair mechanisms. When the DNA damage is too serious, the cell undergoes programmed cell death, or apoptosis. [61]
Comparison	Cisplatin is a widely used chemotherapy drug, but it comes with several significant disadvantages and side effects. It can cause toxicity to the body in many organs. Cisplatin can cause severe kidney damage, which is dose-related and cumulative. Also, Cisplatin can cause hearing loss, which may be irreversible. [62] However, the new drugs KAPI may not have serious side effect. In addition, cancer cells can develop resistance to cisplatin, reducing its effectiveness. This resistance can be caused by various mechanisms, including increased DNA repair and drug efflux. However, those mechanism is not related to the mechanism of KAPI.
Patent	United States Patent Application Publication: Pub No.: US4310515A

Table 4.2 Comparison with Sotorasib

KRAS G12C Inhibitor (Sotorasib)	
Description	Sotorasib is an inhibitor of the RAS GTPase family that binds irreversibly to the P2 pocket in the inactive GDP-bound form of KRAS. It lock the protein in an inactive state. Hence, it blocks KRAS signaling, inhibits tumor growth and promotes cancer cell death. [63]
Comparison	The drug only targets G12C mutation in KRAS. Some patients do not respond to KRAS-G12C inhibitor therapy, mainly due to intrinsic or acquired resistance caused by cellular, molecular, and genetic mechanisms. Hence, the patient that can benefit from the drug is limited. In contrast, KAPI targets PDEδ which facilitate KRAS signalling and this target can affect more type of KRAS mutation and more patients maybe benefited. Also, in the 3-month rat toxicology study, Sotorasib shows notable renal toxicity. It shows that the side effects are of great concern. [64] As peptides drug typically have exquisite potency, selectivity, and low toxicity, it is hoped that our invention can offer more choices for personalized medicine with reduced side effect to non-target tissue. [65]
Patent	United States Patent Application Publication: Pub No.: US 2024/0139193 A1

Table 4.3 Comparison with Keytruda

Pembrolizumab (Keytruda)	
Description	Pembrolizumab is an immunotherapy drug that helps the body's immune system recognize and fight cancer cells by blocking the PD-1 protein on immune cells. When pembrolizumab occupied the PD-1 precisely, it can hinder the combination between PD-1 and its ligands, PD-L1 or PD-L2, to restore the normal anti-tumor immune response suppressed by PD-1 pathway. [66]
Comparison	Serious side effects can occur, such as inflammation of the lungs (pneumonitis). In addition, pembrolizumab can cause the immune system to attack normal organs and tissues in the body, leading to severe and life-threatening complications. [67] However, KAPI's mechanis is not related to the immune system. Hence, such a disadvantage doesn't applied to our peptide drug.
Patent	LU Luxembourg Intellectual Property Office: Pub no: LU92940I2

4.4 Limitation

4.4.1 More evidence should be collected for KAPI's mechanism

In qPCR, the drug's effect on specific cancer signalling pathways related to KRAS was studied. However, PDEδ's binding to KRAS is not yet demonstrated. Moreover, cancer signaling pathway is complicated. KAPI' effect to the signaling pathway should be studied thoroughly while evidence is now limited.

4.4.2 Inhibitory effect of KAPI should be enhanced

In the wetlab experiment, KAPI showed noticeable anti-cancer property toward lung cancer cells. However, the effectiveness of KAPI should be enhanced so that it can work even under very low concentration so as to reduce potential side effects. [68] Selection of in vitro concentrations and in vivo plasma exposures for evaluation of drug effects should be studied.

4.4.3 The duration of drug treatment on 3D MCTS is limited

In this investigation, fusion drug is only incubated with cancer cells for a two-day treatment. The effect of longer treatment has yet to be studied within a limited time. However, chemotherapy drug is not used for a single dose but cycles of treatment.

4.4.4 Pioneer stage in cancer drug development

KAPI hasn't been tested on animals or human bodies directly. KAPI has only been tested in 2D cell culture and on spheroids in lab. However, it is just the beginning of the de novo drug discovery and development, which comprises basic discovery, drug design, in vitro and in vivo experimentation (including identifying safety and efficacy), clinical trials and finally drug registration into the market. [69] Given that KAPI is peptide in nature, it is unsure whether it can maintain its shape and function in the human body. There are many more factors to be considered in the human body that differ from lab testing.

4.5 Future plan

4.5.1 Confirmation of the failure of PDEδ's binding to KRAS by confocal microscopy

In our wet lab experiments, the cytotoxic effect of KAPI on A549 is demonstrated. In qPCR, the drug's effect on specific pathways related to KRAS was studied. Evidence shows that KRAS activity is inhibited under the effect of KAPI. However, this does not directly show whether the cell death is caused solely by the inhibition of KRAS. In order to demonstrate KRAS and PDEδ interaction under the effect of KAPI, confocal microscopy can be used to visualize and compare the co-localization of KAPI and PDEδ using fluorescently tagged versions of both molecules in different concentration of KAPI. [70]

4.5.2 More experimental data should be collected to show KAPI's effect

Apart from the 4 genes targeted in previous experiments (SOS, EGFR, P13K, BRAF), further investigation can be conducted to determine the specific actions of KAPI on KRAS upstream and downstream pathways. For instance, common KRAS downstream pathways and effectors also include RAL-GEF and STAT3, while upstream pathways include GAB 2 and SHP 1 and 2 etc. [71], [72] They are all worth investigating to study the loss of KRAS function. In order to further examine the KAPI's impact on the cancer signal pathway, protein expression of important marker can be studied. [73] Therefore, western blot analysis can be used to measure protein expression in a sample, as well as its abundance and size.

4.5.3 Combination of inhibitor targeting cancer signal pathway

Combining KAPI with other inhibitors targeting cancer signal pathway is one of our future directions. Synergistic effects may be achieved to enhance efficiency and reduce the chance of chemotherapy resistance. For example, SOS1 inhibitors with KRAS inhibitors improved the depth and durability of response in lung and colorectal cancer models. These results highlight the potential of SOS1 inhibitors to broaden the response to KRAS inhibitors in the clinic. [74]

4.5.4 Extended duration of drug treatment on 3D MCTS

At least three successive cycles for 21-day regimen should be conducted for viability assay in a 3D MCTS culture so that the data can be more reliable in terms of chemotherapy duration. [75]Also, the effect of the combined therapy can be studied. Thus, the limitation of being unable to simulate the tumour microenvironment (TME) for a more accurate investigation can be improved with the application of 3D models for the revised ODE model.

4.5.5 Further optimization of the sodium alginate microsphere

Composition of the sodium alginate microsphere can be further studied to optimize the release of KAPI. Studies showed the significance of property of alginate in modulating the rate of drug release in different pH. Also, particle size was found to have an influence on drug release from these matrices as it affects the extent of burst release. Next, higher viscosity of alginate slows down drug release rate. Meanwhile, the type of alginate used is worthy of investigation too. High M-alginate

has a higher ratio of mannuronic acid residues compared to guluronic acid residues. High M-alginate might be more efficient than high-G-alginate in sustaining drug release; and high M-alginate tends to form softer and more flexible gels compared to high G-alginate, which forms stiffer gels. [51]

5. Conclusion

In conclusion, this project successfully developed novel anti-cancer peptides by targeting PDEδ, a regulator of KRAS signaling in cancer cells. Utilizing advanced computational tools such as RFdiffusion, ProteinMPNN, and AlphaFold2, we generated and identified peptide sequences with promising binding affinities. Through the expression of these peptides in the BL21 strain and subsequent testing on the A549 lung cancer cell line, we discovered that ACP5—now designated as KAPI (KRAS and PDEδ Inhibitor)—demonstrated remarkable efficacy, achieving an 80% inhibition of 2D cancer cell viability and a significant impact on 3D Multi-Cellular Tumor Spheroids.

Moreover, the ability of KAPI to enhance the effectiveness of lower concentrations of Cisplatin suggests a potential strategy for reducing the side effects associated with conventional chemotherapy. This study not only highlights the therapeutic potential of AI-generated peptides in cancer treatment but also paves the way for future investigations aimed at optimizing combination therapies for improved patient outcomes. The promising results from KAPI warrant further exploration and validation in preclinical and clinical settings to fully realize its potential in cancer therapy.

Reference:

[1] Datos y Cifras, “Organización Mundial de la Salud. Cáncer.”

[2] M. Goles *et al.*, “Peptide-based drug discovery through artificial intelligence: towards an autonomous design of therapeutic peptides.,” *Brief Bioinform*, vol. 25, no. 4, May 2024, doi: 10.1093/bib/bbae275.

[3] J. Timar and K. Kashofer, “Molecular epidemiology and diagnostics of KRAS mutations in human cancer.,” *Cancer Metastasis Rev*, vol. 39, no. 4, pp. 1029–1038, Dec. 2020, doi: 10.1007/s10555-020-09915-5.

[4] H. J. Kim, H. N. Lee, M. S. Jeong, and S. B. Jang, “Oncogenic KRAS: Signaling and Drug Resistance.,” *Cancers (Basel)*, vol. 13, no. 22, Nov. 2021, doi: 10.3390/cancers13225599.

[5] V. Nancy, I. Callebaut, A. El Marjou, and J. de Gunzburg, “The delta subunit of retinal rod cGMP phosphodiesterase regulates the membrane association of Ras and Rap GTPases.,” *J Biol Chem*, vol. 277, no. 17, pp. 15076–84, Apr. 2002, doi: 10.1074/jbc.M109983200.

[6] D. Uprety and A. A. Adjei, “KRAS: From undruggable to a druggable Cancer Target,” *Cancer Treat Rev*, vol. 89, p. 102070, Sep. 2020, doi: 10.1016/J.CTRV.2020.102070.

[7] G. Zimmermann *et al.*, “Small molecule inhibition of the KRAS-PDEδ interaction impairs oncogenic KRAS signalling.,” *Nature*, vol. 497, no. 7451, pp. 638–42, May 2013, doi: 10.1038/nature12205.

[8] D. Reita *et al.*, “Direct Targeting KRAS Mutation in Non-Small Cell Lung Cancer: Focus on Resistance.,” *Cancers (Basel)*, vol. 14, no. 5, Mar. 2022, doi: 10.3390/cancers14051321.

[9] Y. Yang, H. Zhang, S. Huang, and Q. Chu, “KRAS Mutations in Solid Tumors: Characteristics, Current Therapeutic Strategy, and Potential Treatment Exploration.,” *J Clin Med*, vol. 12, no. 2, Jan. 2023, doi: 10.3390/jcm12020709.

[10] W. H. Abuwatfa, W. G. Pitt, and G. A. Husseini, “Scaffold-based 3D cell culture models in cancer research.,” *J Biomed Sci*, vol. 31, no. 1, p. 7, Jan. 2024, doi: 10.1186/s12929-024-00994-y.

[11] S. El Harane, B. Zidi, N. El Harane, K.-H. Krause, T. Matthes, and O. Preynat-Seauve, “Cancer Spheroids and Organoids as Novel Tools for Research and Therapy: State of the Art and Challenges to Guide Precision Medicine.,” *Cells*, vol. 12, no. 7, Mar. 2023, doi: 10.3390/cells12071001.

[12] E. K. , M.-G. P. , W. H. , W. A. Fansa, “The crystal structure of PDE6D in complex with inhibitor-3,” 2017.

[13] S. A. Ismail *et al.*, “Arl2-GTP and Arl3-GTP regulate a GDI-like transport system for farnesylated cargo.,” *Nat Chem Biol*, vol. 7, no. 12, pp. 942–9, Oct. 2011, doi: 10.1038/nchembio.686.

[14] J. L. Watson *et al.*, “Broadly applicable and accurate protein design by integrating structure prediction networks and diffusion generative models,” *bioRxiv*, p. 2022.12.09.519842, Jan. 2022, doi: 10.1101/2022.12.09.519842.

[15] J. Dauparas *et al.*, “Robust deep learning-based protein sequence design using ProteinMPNN.,” *Science*, vol. 378, no. 6615, pp. 49–56, Oct. 2022, doi:

10.1126/science.add2187.

[16] R. Evans *et al.*, "Protein complex prediction with AlphaFold-Multimer," *bioRxiv*, p. 2021.10.04.463034, Jan. 2022, doi: 10.1101/2021.10.04.463034.

[17] Z. Davoodi and F. Shafiee, "Internalizing RGD, a great motif for targeted peptide and protein delivery: a review article.," *Drug Deliv Transl Res*, vol. 12, no. 10, pp. 2261–2274, Oct. 2022, doi: 10.1007/s13346-022-01116-7.

[18] J. Xie *et al.*, "Cell-Penetrating Peptides in Diagnosis and Treatment of Human Diseases: From Preclinical Research to Clinical Application.," *Front Pharmacol*, vol. 11, p. 697, 2020, doi: 10.3389/fphar.2020.00697.

[19] M. Karami Fath *et al.*, "Anti-cancer peptide-based therapeutic strategies in solid tumors.," *Cell Mol Biol Lett*, vol. 27, no. 1, p. 33, Apr. 2022, doi: 10.1186/s11658-022-00332-w.

[20] Freiburg Bioware09, "Middle Linker (Gly-Gly-Ser-Gly)x2," iGem Registry of Standard Biological Parts (Part:BBa_K243005).

[21] R. Matsumoto, M. Okochi, K. Shimizu, K. Kanie, R. Kato, and H. Honda, "Effects of the properties of short peptides conjugated with cell-penetrating peptides on their internalization into cells.," *Sci Rep*, vol. 5, p. 12884, Aug. 2015, doi: 10.1038/srep12884.

[22] P. K. Lunde *et al.*, "Polyarginine Cell-Penetrating Peptides Bind and Inhibit SERCA2.," *Cells*, vol. 12, no. 19, Sep. 2023, doi: 10.3390/cells12192358.

[23] W. Lu *et al.*, "DynamicBind: predicting ligand-specific protein-ligand complex structure with a deep equivariant generative model.," *Nat Commun*, vol. 15, no. 1, p. 1071, Feb. 2024, doi: 10.1038/s41467-024-45461-2.

[24] P. Buchwald, "A Receptor Model With Binding Affinity, Activation Efficacy, and Signal Amplification Parameters for Complex Fractional Response Versus Occupancy Data.," *Front Pharmacol*, vol. 10, p. 605, 2019, doi: 10.3389/fphar.2019.00605.

[25] Thermo Fisher Scientific, "Preventing edge effect during extended culture in microplates with a unique perimeter moat design," 2017.

[26] E. Oner, S. G. Gray, and S. P. Finn, "Cell Viability Assay with 3D Prostate Tumor Spheroids.," *Methods Mol Biol*, vol. 2645, pp. 263–275, 2023, doi: 10.1007/978-1-0716-3056-3_17.

[27] Thermo Fisher Scientific, "Disease model generation: 5 steps to a 3D cancer spheroid model," 2021.

[28] E. Oner, S. G. Gray, and S. P. Finn, "Cell Viability Assay with 3D Prostate Tumor Spheroids.," *Methods Mol Biol*, vol. 2645, pp. 263–275, 2023, doi: 10.1007/978-1-0716-3056-3_17.

[29] C. A. Schneider, W. S. Rasband, and K. W. Eliceiri, "NIH Image to ImageJ: 25 years of image analysis.," *Nat Methods*, vol. 9, no. 7, pp. 671–5, Jul. 2012, doi: 10.1038/nmeth.2089.

[30] F. Piccinini, A. Tesei, and A. Bevilacqua, "Single-image based methods used for non-invasive volume estimation of cancer spheroids: a practical assessing approach based on entry-level equipment.," *Comput Methods Programs Biomed*, vol. 135, pp. 51–60, Oct. 2016, doi: 10.1016/j.cmpb.2016.07.024.

[31] F. Piccinini, A. Tesei, C. Arienti, and A. Bevilacqua, "Cancer multicellular spheroids: volume assessment from a single 2D projection.," *Comput Methods Programs Biomed*, vol. 118, no.

2, pp. 95–106, Feb. 2015, doi: 10.1016/j.cmpb.2014.12.003.

[32] G. Chen, P. Kronenberger, E. Teugels, I. A. Umelo, and J. De Grève, "Targeting the epidermal growth factor receptor in non-small cell lung cancer cells: the effect of combining RNA interference with tyrosine kinase inhibitors or cetuximab.," *BMC Med*, vol. 10, p. 28, Mar. 2012, doi: 10.1186/1741-7015-10-28.

[33] A. Grothey, M. Fakih, and J. Tabernero, "Management of BRAF-mutant metastatic colorectal cancer: a review of treatment options and evidence-based guidelines," *Annals of Oncology*, vol. 32, no. 8, pp. 959–967, Aug. 2021, doi: 10.1016/J.ANNONC.2021.03.206.

[34] L. Jiang and Z. Tang, "Expression and regulation of the ERK1/2 and p38 MAPK signaling pathways in periodontal tissue remodeling of orthodontic tooth movement.," *Mol Med Rep*, vol. 17, no. 1, pp. 1499–1506, Jan. 2018, doi: 10.3892/mmr.2017.8021.

[35] "Quest Graph™ IC50 Calculator."

[36] Y. Tang *et al.*, "ABCG2 regulates the pattern of self-renewing divisions in cisplatin-resistant non-small cell lung cancer cell lines.," *Oncol Rep*, vol. 32, no. 5, pp. 2168–74, Nov. 2014, doi: 10.3892/or.2014.3470.

[37] M. Biola-Clier *et al.*, "Comparison of the DNA damage response in BEAS-2B and A549 cells exposed to titanium dioxide nanoparticles.," *Mutagenesis*, vol. 32, no. 1, pp. 161–172, Jan. 2017, doi: 10.1093/mutage/gew055.

[38] Barnett Rosenberg, "The 'Accidental' Cure—Platinum-based Treatment for Cancer: The Discovery of Cisplatin," 2014.

[39] C.-Y. Fang *et al.*, "Natural products: potential treatments for cisplatin-induced nephrotoxicity.," *Acta Pharmacol Sin*, vol. 42, no. 12, pp. 1951–1969, Dec. 2021, doi: 10.1038/s41401-021-00620-9.

[40] J. A. Kellum, P. Romagnani, G. Ashuntantang, C. Ronco, A. Zarbock, and H.-J. Anders, "Acute kidney injury," *Nat Rev Dis Primers*, vol. 7, no. 1, p. 52, 2021, doi: 10.1038/s41572-021-00284-z.

[41] M. L. Uribe, I. Marrocco, and Y. Yarden, "EGFR in Cancer: Signaling Mechanisms, Drugs, and Acquired Resistance.," *Cancers (Basel)*, vol. 13, no. 11, Jun. 2021, doi: 10.3390/cancers13112748.

[42] J. Yang, J. Nie, X. Ma, Y. Wei, Y. Peng, and X. Wei, "Targeting PI3K in cancer: mechanisms and advances in clinical trials.," *Mol Cancer*, vol. 18, no. 1, p. 26, Feb. 2019, doi: 10.1186/s12943-019-0954-x.

[43] P. I. Poulikakos, R. J. Sullivan, and R. Yaeger, "Molecular Pathways and Mechanisms of BRAF in Cancer Therapy.," *Clin Cancer Res*, vol. 28, no. 21, pp. 4618–4628, Nov. 2022, doi: 10.1158/1078-0432.CCR-21-2138.

[44] J. Lou *et al.*, "Advances in Oral Drug Delivery Systems: Challenges and Opportunities.," *Pharmaceutics*, vol. 15, no. 2, Feb. 2023, doi: 10.3390/pharmaceutics15020484.

[45] S. Qin *et al.*, "mRNA-based therapeutics: powerful and versatile tools to combat diseases," *Signal Transduct Target Ther*, vol. 7, no. 1, p. 166, 2022, doi: 10.1038/s41392-022-01007-w.

[46] L. Sultatos, “Routes of Drug Administration,” in *xPharm: The Comprehensive Pharmacology Reference*, S. J. Enna and D. B. Bylund, Eds., New York: Elsevier, 2007, pp. 1–3. doi: https://doi.org/10.1016/B978-008055232-3.60070-4.

[47] C. B. Fox, J. Kim, L. V Le, C. L. Nemeth, H. D. Chirra, and T. A. Desai, “Micro/nanofabricated platforms for oral drug delivery.,” *J Control Release*, vol. 219, pp. 431–444, Dec. 2015, doi: 10.1016/j.jconrel.2015.07.033.

[48] M. Nicze, M. Borówka, A. Dec, A. Niemiec, Ł. Bułdak, and B. Okopień, “The Current and Promising Oral Delivery Methods for Protein- and Peptide-Based Drugs.,” *Int J Mol Sci*, vol. 25, no. 2, Jan. 2024, doi: 10.3390/ijms25020815.

[49] S.-J. Cao *et al.*, “Nanoparticles: Oral Delivery for Protein and Peptide Drugs.,” *AAPS PharmSciTech*, vol. 20, no. 5, p. 190, May 2019, doi: 10.1208/s12249-019-1325-z.

[50] P. Biancheri, A. Di Sabatino, G. R. Corazza, and T. T. MacDonald, “Proteases and the gut barrier,” *Cell Tissue Res*, vol. 351, no. 2, pp. 269–280, 2013, doi: 10.1007/s00441-012-1390-z.

[51] C. V. Liew, L. W. Chan, A. L. Ching, and P. W. S. Heng, “Evaluation of sodium alginate as drug release modifier in matrix tablets.,” *Int J Pharm*, vol. 309, no. 1–2, pp. 25–37, Feb. 2006, doi: 10.1016/j.ijpharm.2005.10.040.

[52] M. LASKOWSKI, H. A. HAESSLER, R. P. MIECH, R. J. PEANASKY, and M. LASKOWSKI, “Effect of trypsin inhibitor on passage of insulin across the intestinal barrier.,” *Science*, vol. 127, no. 3306, pp. 1115–6, May 1958, doi: 10.1126/science.127.3306.1115.

[53] B. F. Choonara, Y. E. Choonara, P. Kumar, D. Bijukumar, L. C. du Toit, and V. Pillay, “A review of advanced oral drug delivery technologies facilitating the protection and absorption of protein and peptide molecules.,” *Biotechnol Adv*, vol. 32, no. 7, pp. 1269–1282, Nov. 2014, doi: 10.1016/j.biotechadv.2014.07.006.

[54] K.-J. Kallen and A. Theß, “A development that may evolve into a revolution in medicine: mRNA as the basis for novel, nucleotide-based vaccines and drugs.,” *Ther Adv Vaccines*, vol. 2, no. 1, pp. 10–31, Jan. 2014, doi: 10.1177/2051013613508729.

[55] Y. Shi, M. Shi, Y. Wang, and J. You, “Progress and prospects of mRNA-based drugs in pre-clinical and clinical applications.,” *Signal Transduct Target Ther*, vol. 9, no. 1, p. 322, Nov. 2024, doi: 10.1038/s41392-024-02002-z.

[56] S. F. Dowdy, “Overcoming cellular barriers for RNA therapeutics.,” *Nat Biotechnol*, vol. 35, no. 3, pp. 222–229, Mar. 2017, doi: 10.1038/nbt.3802.

[57] Y. Shi, M. Shi, Y. Wang, and J. You, “Progress and prospects of mRNA-based drugs in pre-clinical and clinical applications.,” *Signal Transduct Target Ther*, vol. 9, no. 1, p. 322, Nov. 2024, doi: 10.1038/s41392-024-02002-z.

[58] J. Reinholz, K. Landfester, and V. Mailänder, “The challenges of oral drug delivery via nanocarriers.,” *Drug Deliv*, vol. 25, no. 1, pp. 1694–1705, Nov. 2018, doi: 10.1080/10717544.2018.1501119.

[59] P. Liu, G. Chen, and J. Zhang, “A Review of Liposomes as a Drug Delivery System: Current Status of Approved Products, Regulatory Environments, and Future Perspectives.,”

Molecules, vol. 27, no. 4, Feb. 2022, doi: 10.3390/molecules27041372.

[60] D. D. Kang, H. Li, and Y. Dong, "Advancements of in vitro transcribed mRNA (IVT mRNA) to enable translation into the clinics.," *Adv Drug Deliv Rev*, vol. 199, p. 114961, Aug. 2023, doi: 10.1016/j.addr.2023.114961.

[61] S. Rottenberg, C. Disler, and P. Perego, "The rediscovery of platinum-based cancer therapy.," *Nat Rev Cancer*, vol. 21, no. 1, pp. 37–50, Jan. 2021, doi: 10.1038/s41568-020-00308-y.

[62] G. Santabarbara, P. Maione, A. Rossi, and C. Gridelli, "Pharmacotherapeutic options for treating adverse effects of Cisplatin chemotherapy.," *Expert Opin Pharmacother*, vol. 17, no. 4, pp. 561–70, 2016, doi: 10.1517/14656566.2016.1122757.

[63] E. C. Nakajima *et al.*, "FDA Approval Summary: Sotorasib for KRAS G12C-Mutated Metastatic NSCLC.," *Clin Cancer Res*, vol. 28, no. 8, pp. 1482–1486, Apr. 2022, doi: 10.1158/1078-0432.CCR-21-3074.

[64] J. Liu, R. Kang, and D. Tang, "Correction: The KRAS-G12C inhibitor: activity and resistance.," *Cancer Gene Ther*, vol. 30, no. 12, p. 1715, Dec. 2023, doi: 10.1038/s41417-023-00692-1.

[65] S. M. Shi and L. Di, "Strategies to Optimize Peptide Stability and Prolong Half-Life," in *Peptide Therapeutics: Fundamentals of Design, Development, and Delivery*, S. D. Jois, Ed., Cham: Springer International Publishing, 2022, pp. 163–182. doi: 10.1007/978-3-031-04544-8_4.

[66] J. Qu *et al.*, "A Review About Pembrolizumab in First-Line Treatment of Advanced NSCLC: Focus on KEYNOTE Studies.," *Cancer Manag Res*, vol. 12, pp. 6493–6509, 2020, doi: 10.2147/CMAR.S257188.

[67] J. P. Flynn and V. Gerriets, *Pembrolizumab*. 2024.

[68] D. R. Liston and M. Davis, "Clinically Relevant Concentrations of Anticancer Drugs: A Guide for Nonclinical Studies.," *Clin Cancer Res*, vol. 23, no. 14, pp. 3489–3498, Jul. 2017, doi: 10.1158/1078-0432.CCR-16-3083.

[69] Z. Zhang *et al.*, "Overcoming cancer therapeutic bottleneck by drug repurposing," *Signal Transduct Target Ther*, vol. 5, no. 1, p. 113, 2020, doi: 10.1038/s41392-020-00213-8.

[70] S. Tovey, P. Brighton, E. Bampton, Y. Huang, and G. Willars, "Confocal microscopy: Theory and applications for cellular signaling," *Methods Mol Biol*, vol. 937, pp. 51–93, Sep. 2012, doi: 10.1007/978-1-62703-086-1_3.

[71] M. Saliani, R. Jalal, and M. R. Ahmadian, "From basic researches to new achievements in therapeutic strategies of KRAS-driven cancers.," *Cancer Biol Med*, vol. 16, no. 3, pp. 435–461, Aug. 2019, doi: 10.20892/j.issn.2095-3941.2018.0530.

[72] Z. Zhu, H. G. Golay, and D. A. Barbie, "Targeting pathways downstream of KRAS in lung adenocarcinoma.," *Pharmacogenomics*, vol. 15, no. 11, pp. 1507–18, Aug. 2014, doi: 10.2217/pgs.14.108.

[73] C. Osborne and S. A. Brooks, "SDS-PAGE and Western blotting to detect proteins and glycoproteins of interest in breast cancer research.," *Methods Mol Med*, vol. 120, pp. 217–29, 2006, doi: 10.1385/1-59259-969-9:217.

[74] “SOS1 inhibitor combinations overcome KRAS inhibitor resistance.,” *Nat Cancer*, vol. 5, no. 9, pp. 1294–1295, Sep. 2024, doi: 10.1038/s43018-024-00801-5.

[75] L. Jiang *et al.*, “Reduction in chemotherapy relative dose intensity decreases overall survival of neoadjuvant chemoradiotherapy in patients with locally advanced esophageal carcinoma,” *BMC Cancer*, vol. 24, no. 1, p. 945, 2024, doi: 10.1186/s12885-024-12724-6.

[76] S. M. Shi and L. Di, “Strategies to Optimize Peptide Stability and Prolong Half-Life,” in *Peptide Therapeutics: Fundamentals of Design, Development, and Delivery*, S. D. Jois, Ed., Cham: Springer International Publishing, 2022, pp. 163–182. doi: 10.1007/978-3-031-04544-8_4.

[77] T. Haider, V. Pandey, N. Banjare, P. N. Gupta, and V. Soni, “Drug resistance in cancer: mechanisms and tackling strategies.,” *Pharmacol Rep*, vol. 72, no. 5, pp. 1125–1151, Oct. 2020, doi: 10.1007/s43440-020-00138-7.

[78] J. Kaiser, “When less is more.,” *Science*, vol. 355, no. 6330, pp. 1144–1146, Mar. 2017, doi: 10.1126/science.355.6330.1144.

[79] L. Jiang *et al.*, “Reduction in chemotherapy relative dose intensity decreases overall survival of neoadjuvant chemoradiotherapy in patients with locally advanced esophageal carcinoma,” *BMC Cancer*, vol. 24, Aug. 2024, doi: 10.1186/s12885-024-12724-6.

[80] Jennifer Welsh, “How Do We Know If Chemotherapy Is Working?,” Verywell Health.

[81] Indranil Mallick, “Response Means in Cancer Treatment,” Verywell Health.

[82] M. Schuler, S. Bölükbas, K. Darwiche, D. Theegarten, K. Herrmann, and M. Stuschke, “Personalized Treatment for Patients With Lung Cancer.,” *Dtsch Arztebl Int*, vol. 120, no. 17, pp. 300–310, Apr. 2023, doi: 10.3238/arztebl.m2023.0012.

Appendix I - ODE model

5.1.1 Introduction

The development of peptide therapeutics is challenging due to their low stabilities and short half-life. However, peptides typically have exquisite potency, selectivity, and low toxicity, making them particularly attractive for disease targets. [76] Hence, concentration and duration of KAPI treatment as chemotherapy require optimization by Mathematical modelling. In this section, we aim to mimic the optimization of chemotherapy using an *in-vitro* culture of A549 Lung Adenocarcinoma.

To model the impact of anticancer peptides KAPI on the growth of cancer cell A549, an Ordinary Differential Equation (ODE) model is used. By employing the ODE model and analyzing the obtained results, the necessary quantity of ACPs to be incorporated to hinder cancer cell growth effectively is approximated. In addition, experimental data collected offers valuable insights into the intricate interactions between KAPI and cancer cell growth. Consequently, these insights can guide the development of the in-vitro cancer cell model.

5.1.2 System of equations in the ODE model

Based on these assumptions, the following equations are constructed:

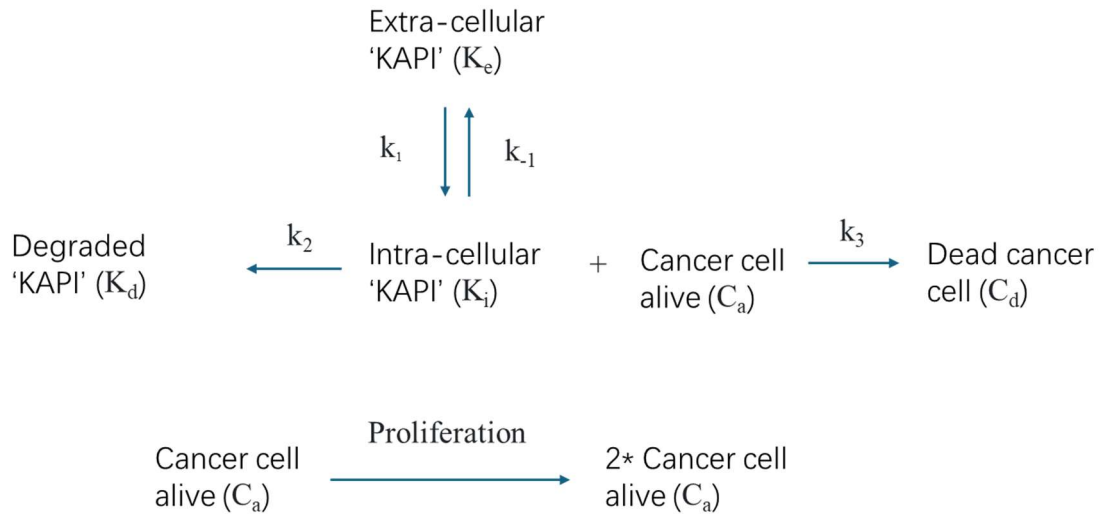

Figure 5.1 Overview of variables and rate constant in the ODE model

The variables involved in the process are as follows:

[Ke]*Ke*	Number of KAPI outside of cancer cell (Extracellular KAPI)
[Ki]*Ki*	Number of KAPI successfully diffused into cancer cell (Intracellular KAPI)
[Kd]*Kd*	Number of KAPI that degraded in a natural manner in cancer cell
[Ca]*Ca*	Number of cancer cells alive
[Cd]*Cd*	Number of dead cancer cells

5.1.3 Construction of the ODE model

- Mathematics behind the model can be assessed from the QR code or link below:
https://kmls-my.sharepoint.com/:b:/g/personal/kwchan_cloud_ktls_edu_hk/ER-tSnLYJlxMqY5olmn83gEBm3W-StTNcVwXb_m-YkourA?e=NKcSeM

5.1.4 Simulation using the ODE model

With the estimated rate constant, the following graphs are constructed by a python program to demonstrate the change in the number of KAPI and cancer cells:

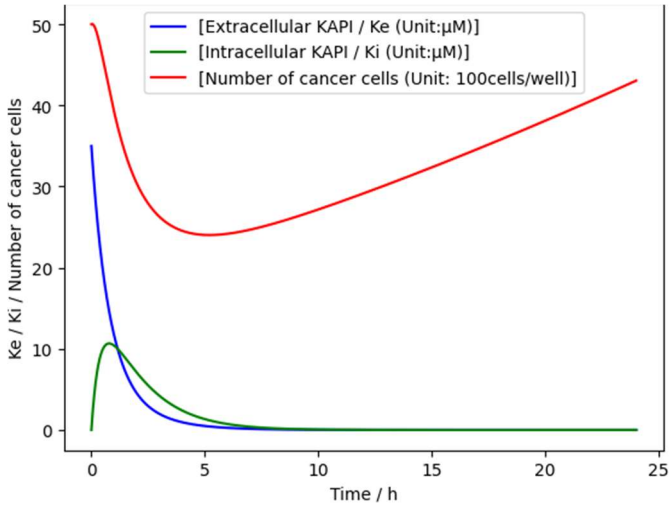

Figure 5.2 ODE model (Initial condition: Number of cancer cells: 5000 cells/well; Concentration of K_e: 35μM, Concentration of K_i: 0μM)

Initially, extracellular KAPI diffuses into the cancer cell. Therefore, when 35μM of KAPI is applied, the concentration of KAPI outside the cancer cell falls drastically after time zero, while the concentration of KAPI inside the cancer cell increases, indicating the diffusion of KAPI into the cancer cell. However, after a duration of less than 5 hours, the concentrations of KAPI inside the cancer cell begin to decline.

In a starting population of 5,000 cancer cells, a sharp decline is observed over time following the administration of KAPI, which demonstrates its capability to inhibit the proliferation of cancer cells. However, the inhibition of cancer growth slowly declines as the concentration of extracellular and

intracellular KAPI drop quickly. After 5 hours, a turning point is reached, marked by an increase in the cancer cell population. This phenomenon reflects the degradation of KAPI, resulting in a loss of its inhibitory function. Consequently, cancer cells can proliferate rapidly, leading to a resurgence in their population.

This scenario highlights the inadequacy of the current quantity of ACPs in effectively suppressing cancer cell proliferation, which occurs at a rapid pace. Therefore, it is imperative to tailor the treatment by adjusting the relevant variables.

5.1.5 Application to the implementation of in-vitro chemotherapy treatment

The focus of our model is to utilize KAPI for inhibition of cancer cell growth, with the challenge from its short half-life inside cells. To determine the appropriate treatment using the ODE model developed, several criteria are considered.

Firstly, the number of KAPI used should be sufficient to inhibit cancer cell viability to an acceptable level after one round of chemotherapy, ensuring an acceptable approach for cancer treatment. Meanwhile, the number of KAPI should be minimized to reduce the development of chemotherapy resistance. Since the development of chemotherapy resistance towards conventional therapy is one of the important reasons for chemotherapy failure in cancer [77] , studies have shown that discontinuous dosing and modifying drug concentrations can combat drug resistance and improve patient survival. [78]

The second consideration is that the concentration of KAPI should be sufficient to effectively suppress the proliferation of cancer cells throughout a treatment cycle, which typically occurs once every three weeks, referred to as a 21-day regimen.[79] Additionally, based on the recommendation of Dr. Lam Ka On during an interview, it is suggested that the objective for reducing cancer cell viability within a treatment cycle should be a minimum of 90%. The interview inspires us to set target for this in-vitro chemotherapy ODE model in a treatment cycle.

In short, the minimum amount of KAPI needed to inhibit the growth of cancer cells in the in-vitro model so that they are kept at an acceptable standard within 504 hours should be found. Then the following graphs are constructed by adjusting the initial value of KAPI to test out different situations for further interpretation.

In Figure 5.3, a partial response is illustrated. A partial response is characterized by a minimum 30% reduction in the total diameters of target lesions, indicating our objective to inhibit 30% of the cancer in this scenario [80], [81]. A $24\mu M$ of KAPI is utilized in the illustration. Following a brief decline, the population of cancer cells exhibits a continuous increase. Concurrently, the depletion of KAPI occurs rapidly. A partial response suggests that the treatment is effective in reducing the

tumor burden, but additional treatment may be necessary to achieve further reduction or control of the cancer cell.

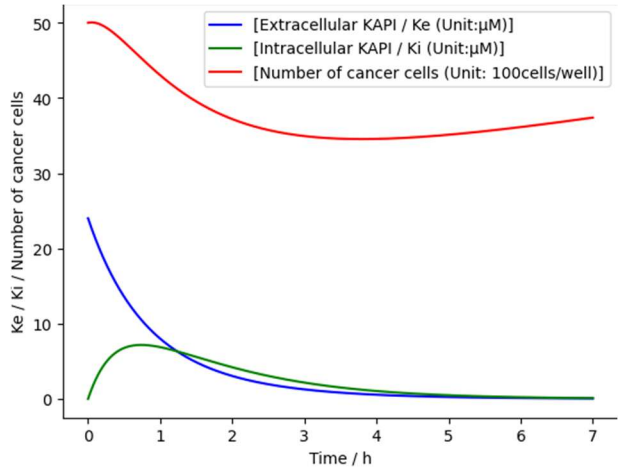

Figure 5.3 Conditions: Number of cancer cell: 5000 cells/ 100μM; Concentration of KAPI: 24μM, Time scale: 7 hours

In Figure 5.4, the time scale is extended to 24 hours. It is shown that cancer cells continue to grow, which reflects that the partial response is not effective, until a frequent drug treatment is implemented.

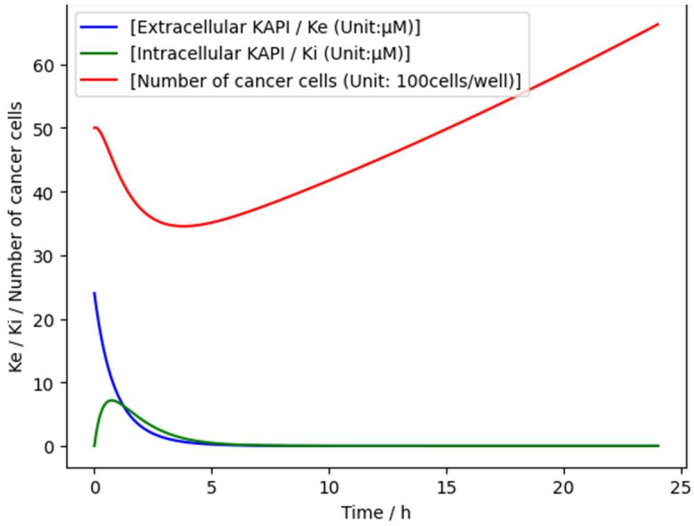

Figure 5.4: Conditions: Number of cancer cell: 5000 cells/ 100μM; Concentration of KAPI: 24μM, Time scale: 24 hours

In Figure 5.5, a significantly elevated quantity of KAPI (100μM) is administered, aiming to achieve complete response. The count of cancer cells diminishes swiftly within the first hour, coinciding with a substantial reduction in the concentration of extracellular KAPI. Following this initial decline, the level of extracellular KAPI decreases at a slower rate.

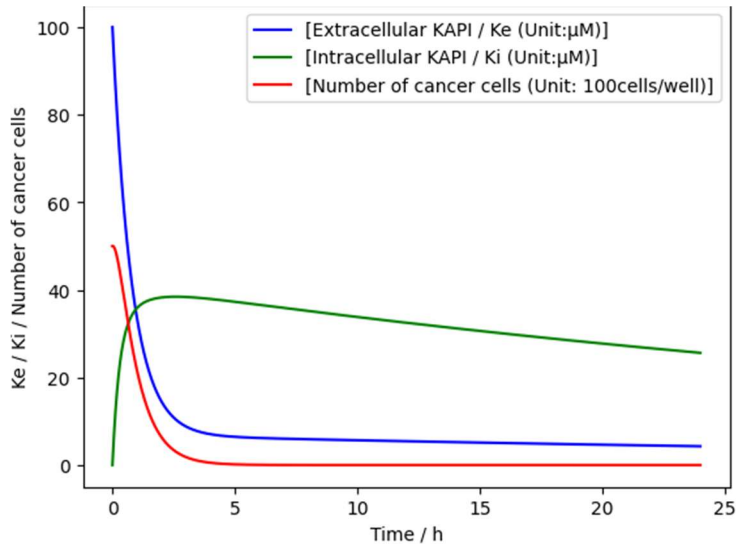

Figure 5.5. Condition: Number of cancer cell: 5000 cells/ 100μM; Amount of KAPI: 100μM, Time scale: 24 hours

In Figure 5.6, it is shown that extracellular KAPI ultimately being depleted by the 200th hour. Regarding intracellular KAPI, it initially rises before experiencing a decline. KAPI stay in the medium and cancer cells for a longer time and ensure no recovery of cancer cells afterwards. Hence, complete response is achieved.

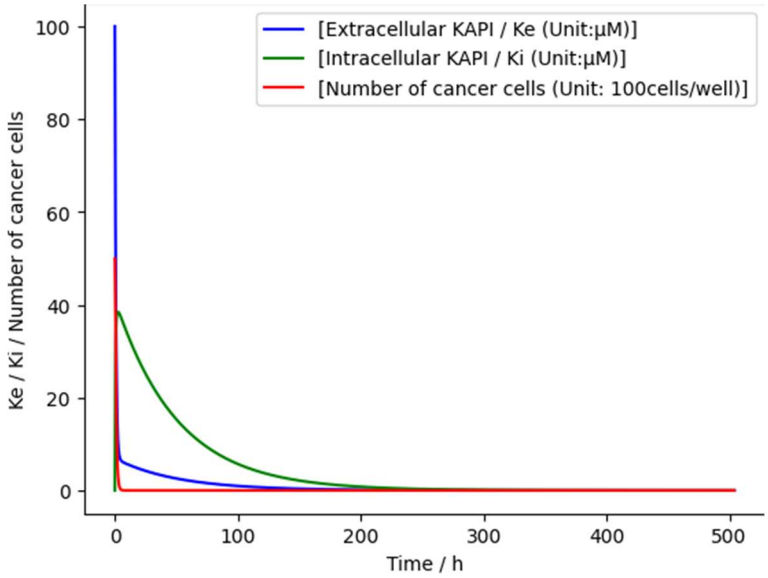

Figure 5.6. Condition: Number of cancer cell: 5000 cells/ 100μM; Amount of KAPI: 100μM, Time scale: 504 hours

Although excess KAPI is effective in eradicating all cancer cells, it is not considered an optimal dosage because of the following reasons:

1. The concentration of drugs used is extremely high, it is likely to induce chemotoxicity, potentially leading to death of the patient.
2. Technical problem may arise due to the production of drugs with a high concentration.
3. It is not financially logical for the extreme overkill.

Hence, the optimal treatment should be achieved. In Figure 5.7, based on the suggestion of Dr. Lam, the starting concentration of KAPI in this scenario is 58μM. It is found that this concentration has been determined to be adequate for achieving a 90% inhibition of the cancer cell population, while maintaining a cancer cell concentration not exceeding 10% of the original number of cancer cells over a period of 252 hours (1.5 weeks). This finding suggests that the specified amount of KAPI is appropriate for a treatment regimen and represents the minimum dosage required to effectively inhibit the proliferation of cancer cells. Hence, this model serves as a significant reference for the application of KAPI in chemotherapy.

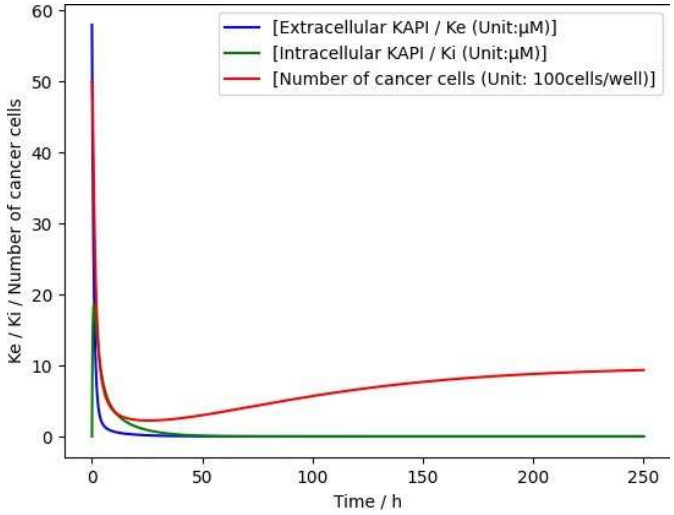

Figure 5.7. Condition: Number of cancer cell: 5000 cells/ 100μM; concentration of KAPI: 58μM

5.1.6 Conclusion

In our study, an ODE model is developed for simulating an in-vitro chemotherapy treatment. In Figure 5.8, an identical optimal concentration of KAPI (58µM) is administered, while the objective is to evaluate its efficacy under different initial conditions, specifically with a starting cell count of 5,500 cells at 59µM. The results indicate that cancer cells exhibit rapid proliferation following a transient decrease. This observation suggests that a uniform dosage of KAPI may not yield consistent outcomes across all patients, given the variability in tumor size. Consequently, the treatment cycle may not adhere to the standard duration, and the 58µM concentration may not be universally applicable. Ultimately, this in-vitro model can be a valuable tool to guide efforts to enhance personalized medicine approach [82] for an elevated efficiency in chemotherapy treatment.

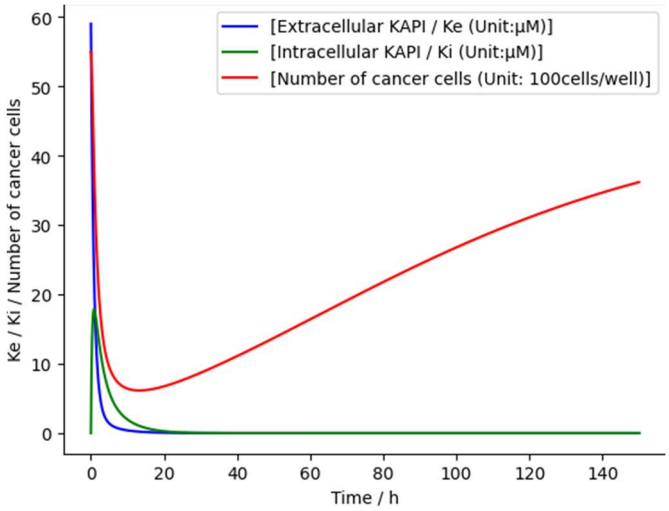

Figure 5.8. Condition: Number of cancer cell: 5500 cells/ 100µM; Concentration of KAPI: 58µM

Appendix II - Educational Promotion

Introduction

Our team has developed a peptide drug named KAPI, which targets PDEδ to inhibit KRAS signaling in lung cancer cells. To promote our findings and engage with the community, a set of game cards (PokeACP) and factsheet is published.

PokeACPs

Card game - The Cancer Killer is designed to engage secondary school students to learn about biotechnology and our project in a fun way. Here are some cards in the game:

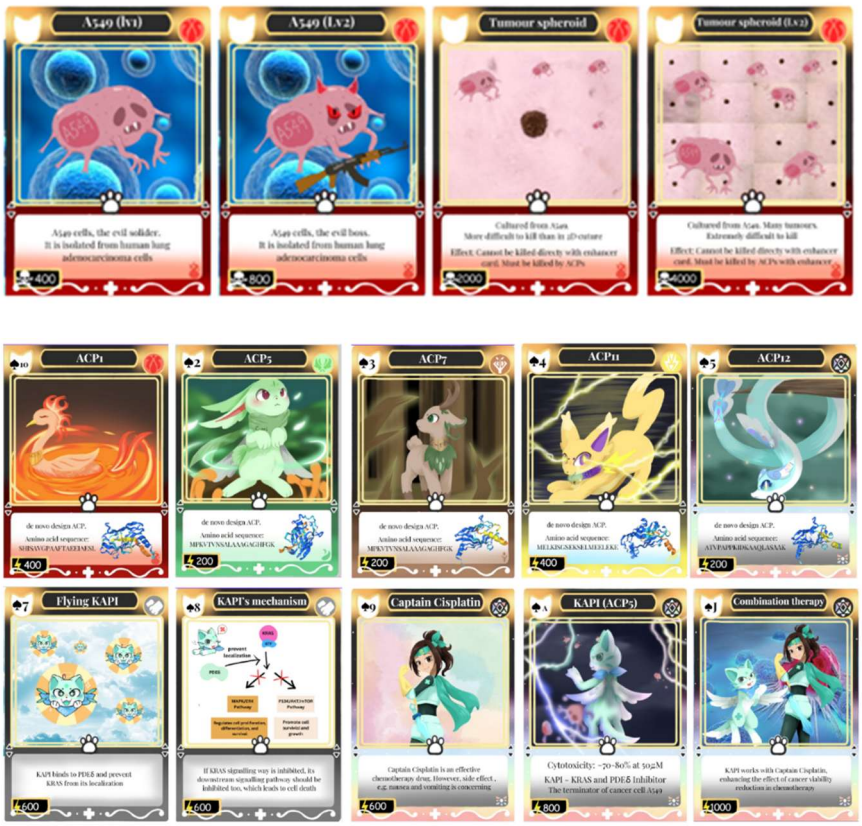

For details of the game rule and our experience in the implementation, please refer to the QR code of link below:https://kmls-my.sharepoint.com/:b:/g/personal/kwchan_cloud_ktls_edu_hk/EQzMog_EqPBBkavVGIUWJEMB_1NESP2USwJ4p6BWHJjn_Q?e=68EEMy

KAPI factsheet

KAPI

KRAS and PDEδ Inhibitor

Peptide drug developed with AI to combat Non-Small Cell Lung Cancer (NSCLC)

Proposed Mechanism

KRAS is one of the most frequently mutated oncogenes in cancer. The oncogenic form of KRAS is able to engage in cytoplasmic signal transduction constantly, most commonly through downstream pathways MAPK/ERK and PI3K, directly resulting in cancer cell survival and abnormal proliferation. KAPI is designated to interfere with the binding of PDEδ to KRAS for suppressing its oncogenic activity by altering its localization to endomembranes. Hence, the ultimate goal is to cause cancer cell death by inhibiting the abnormal KRAS-related cancer signaling pathway.

Structural Modeling

Using AI, de novo peptides were designed to target C56, R61 and Y149 hotspot residues in PDEδ

AlphaFold2 has been utilized to predict the most probable sequences bound to PDEδ, for each predicted PDEδ-peptide complex, a Predict Aligned Error (PAE) is given. It represents the overall distance error of each predicted coordinate, i.e. the distance between the predicted coordinate and the actual coordinate.

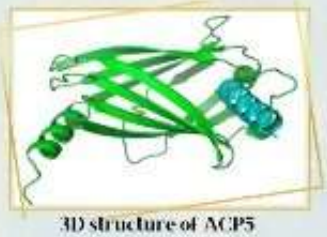

3D structure of ACP5

Plasmids construction and transfromation

The plasmid designed contains an insert of ACP, and is ligated with the pET plasmid. The recombinant plasmid was first transformed in DH5-alpha for cloning. Then, the plasmid was transformed in BL21. Colonies were observed in LB plate with kanamycin. Colony PCR was carried out to confirm whether the bacteria in colony get the correct plasmid

Protein expression

Transformed cell culture was incubated into LB broth containing kanamycin(1X) at 37°C with 150rpm shaking until the OD600 reached 0.6. Then, 0.4mM IPTG was used to induce the protein expression for 24hrs at 20°C. SDS-PAGE was conducted to estimate the protein concentration.

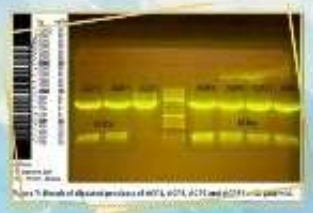

KAPI (KRAS and PDEδ Inhibitor)

Cytotoxicity Test

With a two-day treatment with 25μM and 50μM KAPI, cancer cell culture A549 showed 40% and 80% inhibition in cell viability

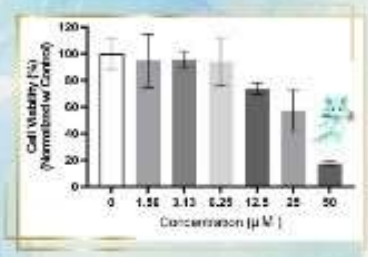

Potential toxicity to normal cells

KAPI shows minimal effect on the cell viability of BEAS-2B (normal human bronchial epithelial cells)

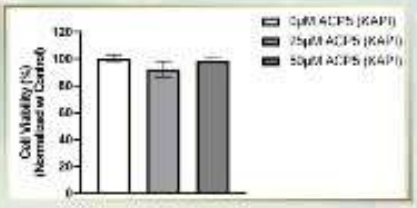

Multi-Cellular Tumour Spheroid (MCTS)

3D spheroids were cultured and selected for cytotoxicity test

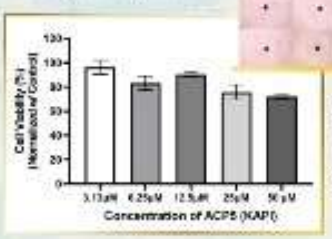

Tumour viability was shown to have a 20% reduction after two-day treatment with 50μM KAPI

Combination Effect

Under the combined treatment with KAPI, less Cisplatin is required to achieve the same degree of inhibition in cancer viability

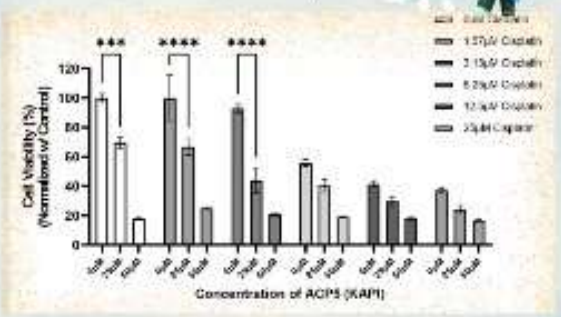

Quantitative Real-Time PCR (qPCR)

Quantitative Real-time PCR was used to compare the mRNA expression patterns of the cancer signaling pathway. EGFR shows up-regulation. It might indicate feedback activation as a response to disrupted downstream signaling in KRAS. Also, both downstream signaling pathway is down regulated, which might indicate a successful disruption of the KRAS signaling pathway

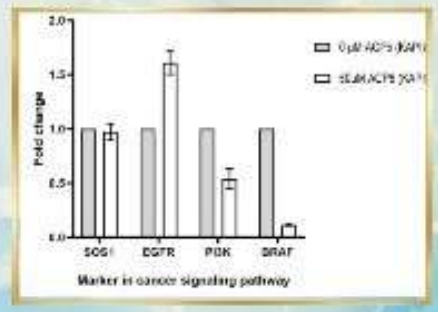

Mathematical Modeling

Using Ordinary Differential Equation, our modeling team determine the optimal treatment for the chemotherapy using KAPI. A minimum dosage of 58μM of KAPI is shown to be able to keep the cancer cell number not to exceed 10% of the initial count over 1.5 weeks, which means the next dose of drug should be administered after this cycle.

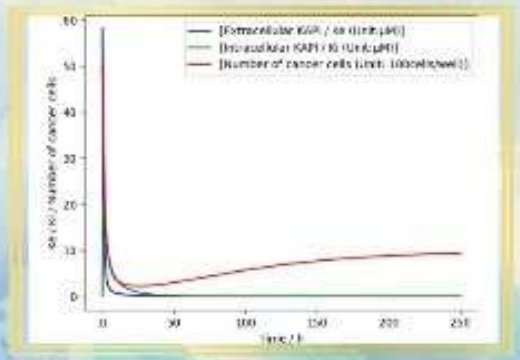

Appendix III – Attribution

May the team express sincere gratitude to many scientists for their invaluable support and guidance.

Interview with Prof. Lo Yuk Ming - Project Optimization

Prove of the mechanism of *de novo* ACP

Prof. Lo suggested that we should do further experiments (e.g. qPCR) to prove the mechanism of our de novo ACPs to ensure they really can block KRAS-PDEδ binding.

Use of control cell lines

He highlighted the necessity of using control cell lines to test the side effects of our drug on normal cells. This step is crucial to ensure the safety and specificity of our peptide drug, minimising potential side effects on healthy tissues.

Research experience and team dynamics

Prof. Lo shared valuable insights from his extensive research experience. He discussed how his team at Novostics approaches scientific projects, emphasizing the importance of collaborative discussions and thorough planning. He encouraged us to adopt similar practices to enhance our research efficiency and outcomes.

Interview with Dr. Lam Ka On- Chemotherapy Drug for Lung Cancer

To gain a deeper understanding in cancer, we turned to the Hong Kong Cancer Fund for guidance. During that time, we had the opportunity to interview Dr. Lam Ka On. His research focuses on innovative treatment approaches and circulating tumour cells related to gastrointestinal and nasopharyngeal cancers, where he has achieved remarkable achievements.

Cisplatin instead of doxorubicin

Dr. Lam provided us with invaluable insights and indicated that cisplatin is one of the most commonly used drugs for targeting lung cancer effectively. This pivotal information allowed us to dismiss the use of doxorubicin, which had been utilised in some of our previous experiments. At the same time, Dr. Lam's endorsement of cisplatin allowed us to confidently confirm that this particular chemotherapy drug would be the focus of our experimental efforts. By making this informed decision, we aimed to ensure that our research would yield more relevant and insightful results in the fight against lung cancer.

Interview with Dr. Liu Bo - Focus to KRAS pathway

We were granted an opportunity to interview Dr. Liu, whose research fields include drug design, and has accumulated rich experience in synthetic research.

Know more about KRAS pathway

Dr. Liu introduced KRAS signalling and KRAS pathway to us since KRAS is one of the commonest gene mutations in cancer. He stressed that KRAS is one of the most common driver mutations in cancer, accounting for 17-25% of all cancers. In non-small cell lung cancer specifically, KRAS mutation has a frequency of around 30%,14% in the form of tumours. This inspired us to focus on KRAS signalling and try out novel approaches to target lung cancer.

These insights can inform and enhance our future research efforts. After the discussion with those experts, we decided to initiate the project of making AI peptides targeting the KRAS pathway. Persuaded by AI nowadays, we wanted to use an AI platform to design some whole new peptides against lung cancer. We hope that all new peptides can have a better anticancer effect with clear mechanisms.

Interview with Dr. Kwong Wai Yeung- Use of AI and 3D Cell culture

We have a precious chance to interview Dr. Keith WY Kwong, founder of the biotech company DreamTec. DreamTec is committed to biotechnology research, innovatively manufacturing cutting-edge products and technologies, focusing on the use of bioengineering, cell Technology and regenerative medicine research.

Use of AI

Dr. Kwong Wai Yeung introduced us to DynamicBind, a powerful tool for predicting binding affinities. He walked us through the steps of setting up simulations, interpreting the results, and comparing binding affinities to identify the most promising peptide candidates. His emphasis on the importance of accurate data interpretation and validation has been invaluable.

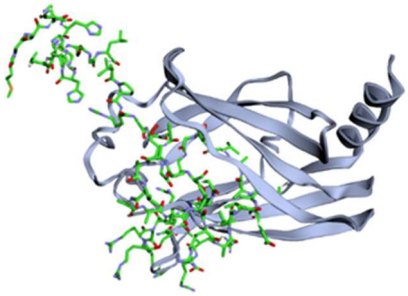

Prediction on the binding affinity of KAPI to PDE

Advantages and Possibilities of 3D Cell Culture

Dr. Kwong highlighted the benefits of 3D cell culture, particularly through spheroid formation, which should be possible for the equipment we have. This method better mimics the in vivo environment compared to traditional 2D cultures. 3D cultures can provide more accurate data on cell behaviour, drug responses, and interactions, making them a valuable tool in cancer research.

Interview with Prof. Mok Shu Kam - Enjoy the Process of Researching

We have a treasurable chance to have an interview with Prof. Mok Shu Kam helping us to understand the current treatment of lung cancer. Prof. Mok is the Li Shu Fan Medical Foundation endowed Professor and Chairman of the Department of Clinical Oncology at the Chinese University of Hong Kong.

KRAS - multiple signalling pathways

He emphasized the importance of the mechanism and the definition of anti-cancer peptides. He pointed out that KRAS has multiple signalling pathways in different forms. We have to know how our drug targeted specific pathways.

Personal experience

Prof. Mok shared his personal experience on doing research on lung cancer treatment as a doctor and a scientist. He discussed the mindset a researcher needs. He reminded us to maintain curiosity about everything and to enjoy the process of researching.

Interview with Mr. Edward Wong – Pain of Cancer

To deepen our understanding of the impact of cancer treatment and the needs of cancer patients, we interviewed Mr. Edward Wong, who was diagnosed with stomach cancer in March 2023. He underwent a total gastrectomy, resulting in the complete removal of his stomach.

Side effects of chemotherapy

During the interview, Mr. Wong shared his experience with several side effects of chemotherapy, including hair loss, dry skin, dysgeusia, vomiting and diarrhoea. These side effects have significantly disrupted his daily life. For instance, he often had to visit the bathroom frequently during the night, which resulted in poor sleep quality. Mr. Wong's experience has reflected how chemotherapy drugs can cast harmful effects on patients, forcing them to confront both physical and emotional hurdles. It calls attention to the imperative need of innovative solutions that aim at reducing chemotherapy side effects, which ignite our passion to tackle the pain for cancer patients.